9

Io's surface composition

Robert W. Carlson, Jeff S. Kargel, Sylvain Douté, Laurence A. Soderblom, and J. Brad Dalton

9.1 INTRODUCTION

The Jovian system presents a panorama of extremes, containing the largest planet in the Solar System surrounded by an equally large and energetic magnetosphere. Orbiting within this magnetosphere is a quartet of planet-sized bodies, the Galilean satellites. The outer three are (water) ice covered bodies. The innermost satellite, Io, differs from the others by being covered by a different kind of ice, frozen sulfur dioxide, and exhibiting the youngest surface in the Solar System, constantly being resurfaced as the most volcanically active body in the Solar System. Incessant tidal kneading heats Io's crust and mantle. This heat escapes through lava flows and eruptions, producing towering volcanic plumes and a dynamic atmosphere. Some plume material escapes to the magnetosphere, forming neutral and ionized belts of gas and plasma around Jupiter and painting neighboring satellites with implanted atoms and ions.

The constantly changing surface is colored from a palette of reds, yellows, greens, grays, white, and black. Fire and ice cover the surface as sulfur, sulfur dioxide, silicates, and unidentified materials derived from plumes, lava lakes, lava flows, fire fountains, and possibly sulfur and sulfur dioxide flows. The surface composition provides clues to the processes that form the surface but also hides information about composition at depth, tantalizing us with puzzling, unidentified colors and spectral features. The observed composition is the result of numerous processes, ranging from initial formation and differentiation, continual cycling of the interior, volcanic activity, plume deposition and redistribution through sublimation, and eventual burial or escape as dust and molecules. In this chapter we summarize what is known and not known about Io's surface composition and some relationships to

volcanic and atmospheric processes. Recent reviews and summaries are given by Geissler (2003), McEwen *et al.* (2004), and Lopes and Williams (2005).

9.1.1 Properties and environment of Io

With a density of 3.53 g cm^{-3}, Io is the highest density object in the outer Solar System and must be composed mainly of silicates, with little H_2O content, if any. Formation models of the Galilean satellites relate the radial decrease in satellite densities (higher ice content with increasing distance from Jupiter) to the radial decrease in Jovian nebula temperatures and ice condensation regions during satellite formation (Lunine *et al.*, 2004; Schubert *et al.*, 2004; see also Chapter 4). However, current models cannot state how much water was incorporated in the newly formed Io. A Jovian nebula snow line beyond Io is consistent with observations but it seems feasible that some water as hydrated silicates was incorporated during formation (Pollack and Fanale, 1982). Almost all such water, if any was accreted, was subsequently lost, because we do not see much water on the surface today. The sulfurous surface indicates that Io formed inside an equivalent condensation front for S-bearing compounds, but the sulfur must have been initially introduced as comparatively refractory metal sulfides, rather than sulfur oxides, because the latter are even more volatile that H_2O.

Galileo radio science results indicate an Fe or Fe–FeS metallic core and at least the outer part should be molten, but there is no internally generated magnetic field (Schubert *et al.*, 2004; see also Chapter 5). The density model suggests a silicate mantle surrounding the core. A recent model finds that the core is completely molten as are portions of the silicate mantle (Keszthelyi *et al.*, 2004). Observed levels of volcanic activity and the corresponding volume of lava relative to the size of Io suggests that each part of Io has been subject to numerous (hundreds) of episodes of melting (Keszthelyi and McEwen, 1997; Keszthelyi *et al.*, 2004), so what we see today is substantially a product of repeated partial melting and crystallization and volatile loss as well as partial recondensation of volatiles on a volcanic surface. This history suggests that there is much uncertainty attached to any estimations of the conditions during the nebula origins of Io or of its initial composition. There have been ample opportunities to generate in Io the most intense igneous and volatile fractionations of any object in the Solar System (Kargel *et al.*, 2003).

Io resides in the heart of Jupiter's powerful magnetosphere and has long been known to interact with it, being bombarded by energetic magnetospheric particles, producing neutral and plasma belts (torii) around Jupiter, and modulating Jupiter's decametric radio emission (see Chapter 11). Io is bombarded by electrons and ions, with the electron component being the most intense. However, the region of electron irradiation is probably limited to the trailing side due to rapid depletion electrons in the flux tubes (Paranicas *et al.*, 2003). The proton flux is more uniform but may be only ~1% of the electron flux (Paranicas *et al.*, 2003). Io also electrically couples to the Jovian upper atmosphere along magnetic flux lines and may be a source of sulfur ions in Jupiter's atmosphere at the foot of the flux tube. Ion and electron sputtering is a major source of atoms, molecules, ions, and dust grains to the magnetosphere. The magnetosphere modifies the surface by radiolysis and implantation, but volcanic and

sublimational resurfacing is rapid so the resulting concentration of radiolytic products may be unimportant. Exceptions may occur on the trailing side, where the flux of energetic electrons is large, or in polar regions, where sublimational resurfacing is slow.

9.1.2 A brief history of Io composition determinations

Io's unusual orange color was recognized by Hertzsprung in 1911 (Kuiper, 1951) and for many years was the reddest object known in the outer Solar System. The darker, redder poles were observed by Minton in 1973 and Murray in 1975 and suggested by Morrison and Burns (1976) to be due to charged-particle irradiation effects since *Pioneer* measurements showed a strong coupling between the magnetosphere and Io (see review by Morrison and Burns,1976; see also Chapter 2). The surface composition was unknown, but absence of an ammonia and methane atmosphere, as possessed by Jupiter, was established by Kuiper (1951). The absence of water ice was first noted by Kuiper in a 1957 abstract, and verified using infrared filter photometry, prism spectrometers, and Fourier transform spectrometers (see review by Johnson and Pilcher, 1977). Much of the early work on Io's surface and atmospheric composition was influenced by the report of post-eclipse brightening (Binder and Cruikshank, 1964), an elusive and yet unverified phenomenon.

Noting that formation models suggested incorporation of hydrated silicates, Fanale and coworkers postulated an evaporate salt surface for Io, where salt-rich water driven from the hot interior evaporates from the surface, leaving bright salt pans (Fanale *et al.*, 1977). Alternatively, Io's low ultraviolet reflectivity prompted Wamsteker *et al.* (1973) to propose sulfur as a constituent based on laboratory measurements although Johnson and McCord had proposed polysulfides in 1971 (Johnson and McCord, 1971). Nelson and Hapke (1978) discussed sulfur allotropes and suggested their presence, possibly produced in volcanic fumeroles, to explain Io's color. Reviews of sulfur on Io and properties of sulfur were given by Sill and Clark (1982) and Nash *et al.* (1986) but significant advances have been made in understanding sulfur subsequent to these reviews. The salt hypothesis was bolstered by the discovery of Io's Na cloud by R. A. Brown in 1974, followed by Trafton's discovery of K in the neutral torus. The notion of sulfur on the surface was boosted by Kupo *et al.*'s (1976) detection of S^+ in the plasma torus (see review by Thomas *et al.*, 2004b).

On the eve of *Voyager*'s first fly-by of the Jupiter system, unidentified bands were found in Io's infrared spectrum (Cruikshank *et al.*, 1978; Pollack *et al.*, 1978; Fink *et al.*, 1978), intense, transient infrared brightening was observed from Io (Witteborn *et al.*, 1979), and tidal heating was predicted that could lead to widespread and recurrent volcanism (Peale *et al.*, 1979). *Voyager* indeed found volcanism (Morabito *et al.*, 1979) and gaseous sulfur dioxide over an active vent (Pearl *et al.*, 1979), leading to the rapid identification of condensed SO_2 as the IR surficial absorber (Hapke, 1979; Fanale *et al.*, 1979; Smythe *et al.*, 1979).

The relatively low temperatures measured by *Voyager*'s IRIS instrument and similarities between Io's colorful, variegated surface and the many colors of sulfur

allotropes suggested the existence of sulfur flows (Sagan, 1979; Pieri *et al.*, 1984) and sulfur volcanism. However, the ductile behavior of sulfur at depths of just a few hundred meters is inconsistent with the kilometer-scale mountains and cliffs on Io (Carr *et al.*, 1979; Clow and Carr, 1980). Ground-based measurements of Io's volcanoes indicated temperatures of ~900 K and, since this temperature is much greater than the 500-K boiling point of sulfur, silicate volcanism was suggested (Johnson *et al.*, 1988). Subsequent measurements showed even higher temperatures, consistent with high-temperature silicate volcanism (see review by McEwen *et al.*, 2000).

During the 16 years between the *Voyager* fly-bys and *Galileo*'s arrival at Jupiter, numerous spectral measurements were obtained from ground-based telescopes, International Ultraviolet Explorer (IUE), International Space Observatory (ISO), and the Hubble Space Telescope (HST). Hot spot monitoring was carried out by Sinton *et al.* (1983). The longitudinal distribution of surficial SO_2 was measured by IUE (Nelson *et al.*, 1980; Nelson *et al.*, 1987) and ground-based infrared spectroscopy (Howell *et al.*, 1984) while SO_2 maps were derived from *Voyager* and HST images. Additional features were found in ground-based infrared spectra, prompting extensive laboratory work and numerous suggestions for spectral identifications (discussed later). High-resolution spectra of Io were obtained by Schmidt *et al.*'s ISO observations (see Schmitt and Rodriguez, 2000). Eleven years after *Voyager*'s discovery of SO_2 in the atmosphere, Lellouch *et al.* (1990) obtained microwave measurements of atmospheric SO_2, followed by Ballester *et al.*'s (1994) ultraviolet measurement of atmospheric SO_2 from HST. Atmospheric SO was later observed by Lellouch *et al.* (1996) and NaCl was observed in volcanic plumes, finally resolving the puzzle of Io's sodium source (Lellouch *et al.*, 2003). Plume modeling by Zolotov, Fegley, and co-workers provided insight into surface composition and volcanic plumes. A pre-*Galileo* summary of Io spectroscopy and surface composition is found in Nash and Betts (1998) and a pre-*Galileo* review of Io was presented by Spencer and Schneider (1996).

Formation of the *International Jupiter Watch* in 1990 (Russell *et al.*, 1990), with monitoring of Io through its *Io Watch* component, provided temporal coverage of time-variable phenomena in the Jovian system to complement the forthcoming *Galileo* measurements. These important ground-based and Earth-orbiting measurements continued throughout *Galileo*'s observational phase and still continue today.

Galileo arrived at Jupiter in December 1995 and carried infrared and ultraviolet spectrometers for compositional mapping (near-infrared mapping spectrometer (NIMS) and ultraviolet spectrometer (UVS)), a photopolarimeter and radiometer instrument (PPR) for thermal measurements, and a camera with narrow and wide-band filters (solid-state imaging system (SSI)). Additionally, various fields and particle instruments that provided *in situ* compositional data in the vicinity of Io as well as magnetic field and plasma wave measurements. The *Galileo* mission and its experiment complement are described in a volume of *Space Science Reviews* (Russell, 1992; see also Chapter 3). Remote-sensing observations during the Io fly-by at Jupiter orbit insertion were precluded due to problems with the spacecraft's tape recorder and no close encounters with Io occurred during the prime mission, limiting the spatial resolution of Io observations during that period. Following the prime mission,

two extended missions did provide numerous close fly-bys of Io. Unfortunately, spectral scanning in the NIMS instrument became inoperative due to radiation damage prior to the first of the close Io fly-bys, so contiguous spectra of Io at high spatial resolution were never obtained by NIMS. This limitation severely degraded the NIMS search for silicate minerals, but thermal and compositional mappings (SO_2) were performed with the remaining fixed-wavelength channels. Despite the low data rate from loss of the high-gain antenna, the *Galileo* data set has high science content and more discoveries are expected from continued analysis of these and Earth-based observations.

9.2 SPECTROSCOPIC DETERMINATIONS OF IO'S COMPOSITION

9.2.1 Overview

Compositional information is derived from numerous sources, including surface reflection and thermal spectroscopy, emission spectroscopy from the atmosphere and torus, x-ray spectroscopy, and *in situ* plasma and plasma wave measurements. Reflectance spectroscopy is the most widely exploited technique, performed from ground-based and Earth-orbiting telescopes and from the *Galileo* spacecraft in Jupiter orbit. As a summary and introduction to the discussion that follows, reflectance spectra of Io, adopted and extended from the compilation by Spencer *et al.* (2004), are shown in Figure 9.1 with diagnostic spectral features delineated in Table 9.1 and discussed below.

The ultraviolet region shows absorption features from atmospheric and surficial SO_2 in the 200–240-nm region and a longer wavelength band from condensed SO_2 centered at 280 nm. There could be some absorption from S_8 and polymeric sulfur S_∞ as well. The edge at 330 nm is indicative of SO_2. For the visible region, the edge extending from 400–500 nm is characteristic of sulfur although disulfur monoxide and polysulfur oxide (PSO) have also been attributed to this absorption. An absorption feature at 560 nm is attributed to tetrasulfur S_4. Io's dark caldera material exhibits an absorption feature at 890 nm that has been attributed to iron-containing silicates. The broad rise between $\sim$1 μm and $\sim$2 μm in the infrared is unexplained; candidate absorbers are Fe-containing silicates or salts, sulfides, impure sulfur, or sulfur polymers. From 1.98 μm to 5.2 μm, most of the features are due to sulfur dioxide including isotopic bands. The feature at 3.15 μm is apparently not due to SO_2; H_2O has been suggested as the absorber and oxyhydroxides are possible. An absorption band at 3.94 μm, superimposed on an SO_2 absorption plateau, has been suggested to be due to H_2S or, more recently, Cl_2SO_2 and $ClSO_2$. Thermal emission spectra (Figure 9.4) show evidence for S_8, SO_2, possibly SO_3, and perhaps others. Spectra of Io's plumes (not shown) indicate sulfur (S_2) and sodium chloride. Emission spectra of the Io torus (not shown) indicate that Na, K, and Cl atoms are being ejected from the surface or plumes, along with sulfur and oxygen. The above constituents and other plausible candidates that have been suggested are discussed below.

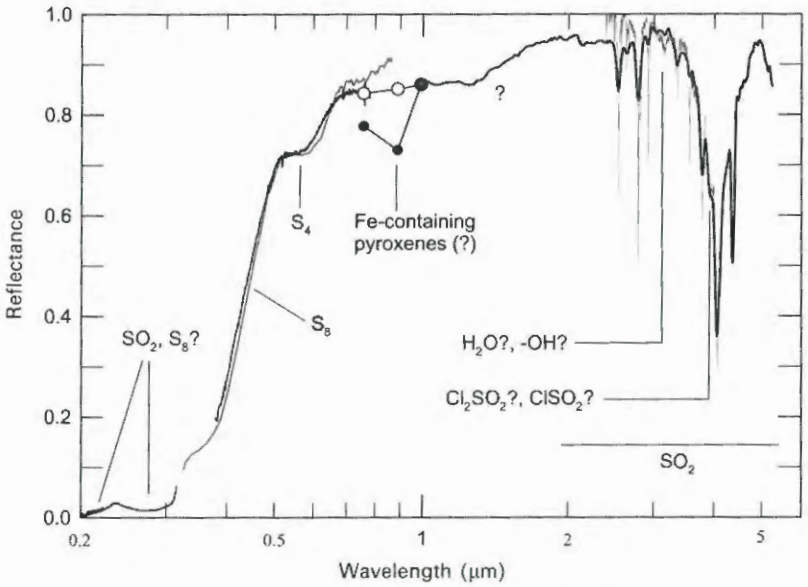

Figure 9.1. Solar reflectance spectra of Io. The ultraviolet HST measurements in the 200- to 310-nm region are from Jessup *et al.* (2002); ground-based measurements from 330–860-nm data (blue line; see also color section) and from 380–780 nm (black line) are from Nelson and Hapke (1978) and Spencer *et al.* (1995), respectively. Scaled *Galileo* SSI multicolor spectrophotometry of white areas (open circles) and dark areas (filled circles) are from Geissler *et al.* (1999). Modest resolution near-infrared measurements by *Galileo* NIMS (black line) are from Carlson *et al.* (1997) while the higher resolution ISO spectrum (red line) is from Schmitt and Rodriguez (2003). Many of these spectra are summarized in the compilation by Spencer *et al.* (2004).

9.2.2 Sulfur

Properties of sulfur

There has been considerable progress in elucidating the properties of sulfur in the past two decades, summarized recently in several articles in two volumes (Steudel, 2003a, b). Since sulfur is an important component of Io's surface, we summarize its properties using the above-mentioned reviews, along with the review by Sill and Clark (1982) and original research papers.

Physical properties. Sulfur can exist in many different sizes of molecular clusters S_n, generally as chains (catena-S) or rings (cyclo-S). Small sulfur molecules, where $n = 2$, 3, or 4, form chains whereas molecules with $n = 6$ to at least 20 form rings. The $n = 5$ molecule can produce either chains or rings, but the lowest energy state is the ring form. A number of isomers are possible for each n. The ring structures are more stable than chains, and molecules with an even number of sulfur atoms are more stable than those with odd numbers of molecules.

Table 9.1. Io's spectral features with known or suggested identifications of surface species and related atoms and molecules.

Type of spectrum	Wavelength, wavenumber, or spectral region	Identifications and suggestions	Notes
Solar reflectance	200–300 nm	SO_2, possible S_8, S_∞	Primarily SO_2
Solar reflectance	350–500 nm	Absorption edge; S_8, S_∞, possible polysulfur oxides (PSO)	$S_8(\beta)$ likely
Solar reflectance	~560 nm	S_4, but Na_2S, S_2O, Cl_2S, and color-centers also suggested	S_4 most likely
Solar reflectance	~900 nm	Fe-containing orthopyroxene (enstatite)	No olivine
Solar reflectance	1–1.6 μm	Fe-containing salts, feldspars, FeS_2, polymeric S (S dangling bonds) sulfur with impurities	Ubiquitous feature, enhanced in southern polar region, depleted in Pele plume deposit
Solar reflectance	1.98–5 μm	SO_2	Ubiquitous frost
Solar reflectance	3–5 μm	H_2SO_3 suggested for some SO_2 bands	Production rate extremely small compared with resurfacing rate
Solar reflectance	3.15 μm	H_2O in SO_2, mineralic OH, HCl	Enhanced concentration in bright equatorial SO_2 snowfields
Solar reflectance	3 μm	H_2O?	Localized feature
Solar reflectance	3.92 μm	H_2S (?), Cl_2SO_2 (?)	H_2S unstable on Io
Mid-infrared thermal emission (*Voyager*)	400–600 cm^{-1}	S_8, SO_2, SO_3, S_2O rings	Detailed analysis unpublished. See Figure 9.4.
Plume spectra	Ultraviolet, visible, microwave	S_2, SO, NaCl, KCl (possible)	Powerful method for Io composition studies
Exosphere and torii emission spectra	Various	Neutral Na, K, Cl, S, SO and ions of O, S, Cl	Upper limits for other species given by Na *et al.* (1998)
Plasma wave features	Ion cyclotron	SO2, SO, H2S, Cl, S ions	H_2S signal sporadic, noisy

In the vapor phase, between 473 K and 1,273 K, molecules with 2–10 atoms are formed and some of these molecules exist as two different isomers (S_4 in particular). At low temperatures, the cyclic S_8, S_7, and S_6 forms dominate, but at higher temperatures S_3 and then S_2 are the most abundant. S_4 is most abundant at 900 K (Steudel *et al.*, 2003).

Liquid sulfur at low temperature contains rings with 6 to at least 35 atoms and probably even larger rings and polymers, denoted S_∞. Above 523 K the small chains S_2, S_3, S_4, and S_5 are also present.

In the solid state many of these allotropes form one or more stable crystals. For example, the most stable form of sulfur is S_8, the cyclo-octal form sometimes called λ-S, which can crystallize into orthorhombic and two different monoclinic forms, denoted $S_8(\alpha)$, $S_8(\beta)$, and $S_8(\lambda)$, respectively. High molecular weight sulfur molecules, polymeric sulfur, denoted S_μ or S_∞, form long chains and probably contain large ringed molecules as well. The α-form of S_8 is the only thermodynamically stable form below 367 K and assemblages of the more unstable molecules eventually revert to $S_8(\alpha)$ at annealing rates that are not well established. $S_8(\beta)$ can be long-lived below 198 K. The polymeric form S_∞ and $S_8(\beta)$ have been studied by Moses and Nash (1991), who showed that these forms can exist as long-lived metastable species on Io.

Solid sulfur phases are bound by Van der Waals forces so the crystals are friable and have low melting points. The melting points for $S_8(\alpha)$ and $S_8(\beta)$ are about 388 K and 393 K, respectively (Eckert and Steudal, 2003).

Spectroscopic properties. The S_2 molecule absorbs in the Schumann–Runge band $B^3\Sigma_g^- \leftarrow X^3\Sigma_u^-$ from the ultraviolet to 500 nm or greater, with the band origin occurring at 316 nm, and appears pale violet in the vapor state (Meyer *et al.*, 1972; Eckert and Steudal, 2003). S_3 has an absorption band with diffuse structure centered at 400 nm and extending to ~500 nm. S_4 exhibits two continua, a band centered at about 530 nm and absorbing between ~460–590 nm that is attributed to the C_{2v} isomer and a weaker band of the C_{2h} form at 625 nm (Meyer *et al.*, 1972; Eckert and Steudal, 2003). It is the 530-nm S_4 (C_{2v}) system that causes sulfur vapor to appear red (Meyer *et al.*, 1972). The molar extinction coefficient for S_3 is ~ 10× that of S_4. Weak bands around 750 nm are observed in the vapor but their origin is unknown (Meyer *et al.*, 1972). S_8 vapor shows a strong absorption band at ~280 nm, a minimum or inflection point at 245 nm, and a stronger band extending down to 210 nm and below (Bass, 1963).

The red absorbing tetrasulfur S_4 can be formed during co-deposition of S_2+Kr when $S_2 : Kr > 1 : 200$, forming a red film. Films of S_2 in Kr produced with lesser amounts of S_2 yield S_4 when irradiated with visible light (Meyer and Stroyer-Hansen, 1972). Annealing of S_2 in a Kr matrix also produces the 530-nm feature of S_4 (Meyer *et al.*, 1972).

Liquid S_8 at its melting point (393 K) is yellow due to the strong ultraviolet absorption and vibrational broadening that extends the wing of the absorption band into the blue end of the visible spectrum. As the temperature rises, the absorption shifts to longer wavelengths and other catena-S and chained-S contribute to the absorption. Between 573–973 K, the 400-nm absorption band of S_3 becomes

apparent, and this band and the 530-nm band of S_4 (C_{2v}) are found between 773–1,173 K. The deep red and red–brown color of liquid sulfur above 673 K has been attributed to a mix of greenish-yellow S_3, the purple–red S_4, and short-chains that can absorb at longer wavelengths. For temperatures >673 K, the increased density of chain radicals produces an absorption band at ~950 nm due to excitation of the chain ends – dangling bonds (Hosokawa *et al.*, 1994; Eckert and Steudal, 2003). The absorption can extend to 1.3 μm and beyond.

Condensed sulfur vapor and quenched sulfur melts frozen at low temperatures exhibiting various colors ranging from black, green, or red that arise from small molecules and radicals trapped in the solid (Eckert and Steudal, 2003). Vapor condensed at 77 K is yellow for furnace temperatures of 415–475 K, green for temperatures of 475–550 K, olive green at 550–800 K, and purple for 800–1,200 K. The purple color changed to olive green when the sample's temperature was elevated from 77 K to 195 K. All films except the purple ones were stable at 195 K (Meyer *et al.*, 1971; Eckert and Steudal, 2003; Radford and Rice, 1960; Chatelain and Buttet, 1965). Quenched red sulfur is metastable at 77 K and converts to yellow polymeric sulfur at 194 K (Meyer *et al.*, 1971).

In the solid phase, cyclic and polymeric sulfur compounds absorb strongly in the ultraviolet with a wing extending into the visible due to thermal excitation of ground-state vibrational levels and, for S_8, phonon-assisted indirect transitions (Eckert and Steudal, 2003). This absorption causes these molecules to appear yellow at room temperature and, if not exposed to ultraviolet radiation (see below), they become white (for S_8, S_{12}, S_{20}) or light yellow (S_6, S_7, S_{10}) at Io-like temperatures (Eckert and Steudal, 2003). Absorption spectra of S_8 and polymeric S show an absorption maximum at ~275–280 nm, an absorption minimum at 250 nm, and strong absorption at shorter wavelengths, similar to the absorption properties of S_8 vapor (Nelson and Hapke, 1978; Sill and Clark, 1982). Sulfur is so absorbing below 400 nm that the reflection properties of most allotropes resemble metals, yielding a flat reflectance spectrum from Fresnel reflection. The 350–500-nm absorption profiles of $S_8(\beta)$ and S_∞ differ somewhat from the S_8 profile (Moses and Nash, 1991). Impurities in sulfur can also alter the absorption and spectral properties (see below).

Raman and infrared spectra are reviewed by Eckert and Steudal (2003) for many allotropes. The infrared-active lines of $S_8(\alpha)$ include the bending transitions at 190–200 cm^{-1} and 240 cm^{-1} and stretching transitions in the 465–480 cm^{-1} region. The infrared spectrum of $S_8(\beta)$ is not available. Polymeric sulfur S_∞ exhibits a strong band at 460 cm^{-1} and a weaker one at 423 cm^{-1}.

Photolytic and radiolytic properties. Under ultraviolet photolysis, white S_8 at 77 K turns yellow (Steudel *et al.*, 1986; Hapke and Graham, 1989), possibly due to generation of S_3. Other allotropes become intense yellow (S_7, S_{10}), grayish-yellow (S_{12}, S_{20}, S_∞), or brownish-yellow (S_6). S_8 stays yellow while the allotropes revert to normal yellow upon heating to room temperature. The timescale at Io's illumination level is a few hours to establish color, and up to a few weeks to achieve equilibrium (Steudel *et al.*, 1986). Photolysis of S_8 in solutions produces bands at 325, 420, 530, and 600 nm (Casal and Scaino, 1985; Nishijima *et al.*, 1976). These are likely from S_3

(400-nm band) and S_4 (530- and 600-nm bands), suggesting that S_8 photolyzes to S_3+S_5 and S_4+S_4. The band at 325 nm may arise from the S_5 molecule but its absorption spectrum is unknown (Eckert and Steudal, 2003).

Energetic electrons and ions bombarding Io's surface will initiate chemical reactions and produce new molecules. These radiolytic reactions are approximately independent of the specific type of ionizing radiation (e.g., electrons, ions, γ-rays, x-rays). Proton irradiation of S_8 at 20 K produces multicolored samples that become black–brown–dark brown at 144 K (Moore, 1984). Under γ-ray irradiation S_8 turns deep red or red–brown and this color remains stable only at low temperature, rapidly reverting to yellow upon warming to room temperature (Radford and Rice, 1960). Nelson *et al.* (1990) performed x-ray irradiations of S_8 and found absorption bands at 420 and 520 nm, consistent with the formation of S_3 and S_4. The 420-nm S_3 feature disappears upon warming to 180 K, but the 520-nm feature remains, reduced somewhat in strength. S_3 produced in an electric discharge disappears when warmed to 130 K while S_4 disappears between 130 and 180 K, producing S_8 (Hopkins *et al.*, 1973). Photolytically produced S_4 has a lifetime of ~60 hours at 171 K (Meyer and Stroyer-Hansen, 1972). Sputtering of S_8 yields mainly S_2 but atomic sulfur and all molecules up to S_8 are present at the ~10% level (Boring *et al.*, 1985; Chrisey *et al.*, 1988).

Impurities in sulfur. As with ice, quartz, and many other minerals, optical transmission into, and scattering from, the interiors of sulfur crystals enables disseminated absorbers (impurities) to modify the effective reflectance spectra of dirty sulfur. This effect has been noted for natural sulfur samples (Kargel *et al.*, 1999) and is further indicated in Figure 9.2 for the case of laboratory controlled disseminations of pyrite (FeS_2) in sulfur (Kargel *et al.*, 2000; MacIntyre *et al.*, 2000). The pyrite imposes differing spectroscopic effects depending on both its grain size and its abundance, and also on the grain size of the sulfur.

Trace amounts of other types of impurities can have even more drastic effects on the spectral properties of sulfur if the impurity either ruptures the polymeric bonds in sulfur or tangles them. In general, elements close to sulfur in the periodic table of the elements have an affinity for sulfur, but unlike chalcophile transition metals (such as Fe, Ni, Cu, and Mn), these elements also have significant solubilities in molten sulfur. The strong chalcophile affinities of many elements has been noted in analyses of natural sulfur samples (Kargel *et al.*, 1999). When these molten mixtures crystallize, the impurities commonly attach to the ends of polymer chains or intrude within them, thus modifying the polymeric state and other physical properties of the sulfur. Since polymer chain length can be large, even small amounts of these impurities can have a large effect on polymerization and spectral reflectivity. This is shown in the case of tellurium in sulfur in Figure 9.3 (Kargel *et al.*, 2000; MacIntyre *et al.*, 2000).

Sulfur on Io

Wamsteker *et al.*'s (1973) suggestion for sulfur on Io was based on the similarity of the 350–500-nm absorption edge, prominent in Io's spectrum, to laboratory reflectance spectra measured by Sill (1973). Sulfur was also thought to be consistent with the

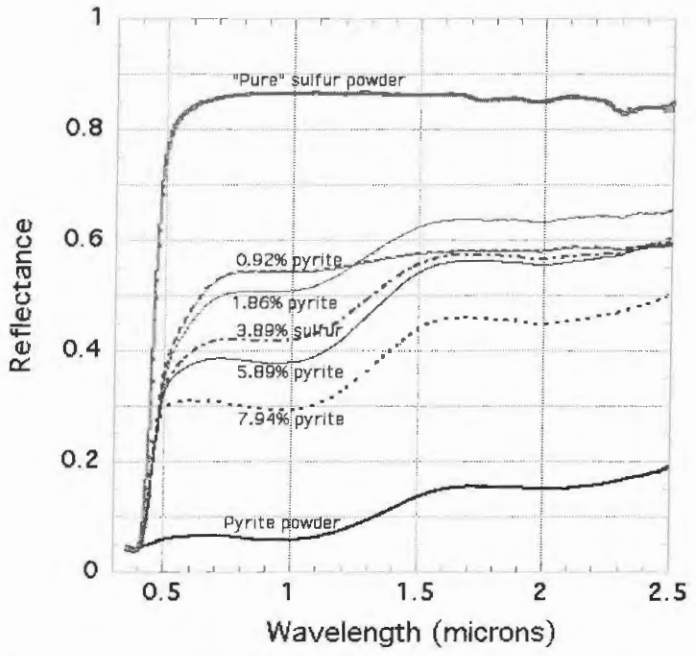

Figure 9.2. Spectra of sulfur with pyrite at various concentrations.

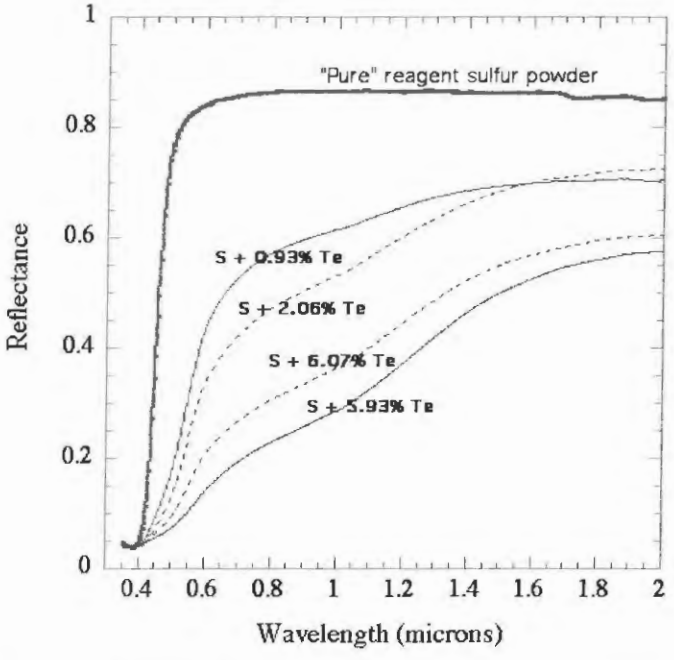

Figure 9.3. Spectra of sulfur with tellurium at various concentrations.

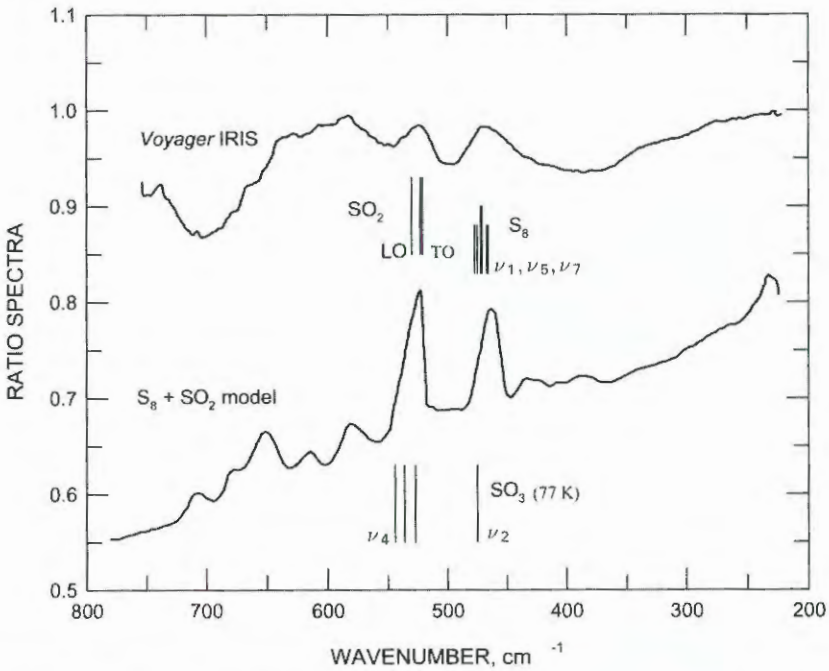

Figure 9.4. *Voyager* thermal emission spectrum of Io and model. The thermal emission spectrum is an average of 78 spectra, divided by an estimated thermal (black body) background. The model is for an unspecified $S_8 + SO_2$ mixture. The positions of fundamental S_8 and SO_2 absorptions are indicated as well as those for the strongest SO_3 bands. The data and model are from Hanel *et al.* (2003).

putative post-eclipse brightening arising from temperature drops during eclipse that shift the sulfur absorption edge to shorter wavelengths, causing the net albedo to be larger when the satellite emerges from eclipse. However, this color effect was not found in *Galileo* images of Io (Simonelli *et al.*, 1994), perhaps due to the presence of non-$S_8(\alpha)$ allotropes that show less color change with temperature (Moses and Nash, 1991). Furthermore, Steudal *et al.* have shown that exposing S_8 for a few days at Io's ultraviolet irradiation level produces a yellow-colored form of sulfur whose color is then insensitive to temperature changes (Steudel *et al.*, 1986). Nelson and Hapke's (1978) ground-based spectrophotometry showed the 400–500-nm edge, an absorption band at 560 nm, and an absorption edge at 330 nm. The latter was attributed to mixtures of sulfur allotropes, but SO_2 absorption provides a better explanation (Nelson *et al.*, 1987; Nelson *et al.*, 1980). Io's 560-nm feature, previously suggested to be from ferric iron (Nash and Fanale, 1977) or color centers in evaporite salts (Fanale *et al.*, 1974, 1977) was identified for the first time with S_4 by Nelson and Hapke (1978).

Additional evidence for elemental sulfur on Io was found in *Voyager* IRIS thermal emission spectra (Figure 9.4; Pearl, 1988; Hanel *et al.*, 2003). Two

features were observed, a band at 525 cm^{-1}, attributed to SO_2, and a band at 470 cm^{-1}, tentatively assigned as the ν_5 band of S_8 (Pearl, 1988) although infrared-active bands of ν_7 and ν_1 transitions can also contribute to the 470-cm^{-1} complex (Eckert and Steudal, 2003). The model fit of Figure 9.2 assumed a temperature decrease with depth of 25 K $cm\ 1^{-1}$. No abundances were given (although S_8 is apparently more abundant than SO_2, see Moses and Nash, 1991) and no definitive analysis has been published so this identification remains tentative.

The first spectroscopically definitive measurements of elemental sulfur at Io were the observations of atomic and molecular sulfur (S_2) in the Pele plume by McGrath *et al.* (2000) and Spencer *et al.* (2000).

The existence of sulfur on Io has been proven but the abundance remains in question. Early objections to the presence of massive amounts of sulfur by Young (1984) were based on the white appearance of $S_8(\alpha)$ at Io's temperature, contrary to Io's orange–yellow appearance. This argument was countered by Moses and Nash (1991) who showed that other allotropes ($S_8(\beta)$ and S_∞) that match Io's reflectance spectrum (and color) can be long-lived under Io conditions. Additionally, the rapid ultraviolet yellowing of sulfur at Io-like temperatures found by Steudal *et al.* (1986) negates Young's color argument. Young further suggested that the chromophores S_3 and S_4 would be unstable on Io. Based on the above discussions of S_3 and S_4 this is certainly true for S_3 and there are no spectral features from Io that suggests its presence there. The S_4 (C_{2v}) molecule that likely provides at least some of Io's red tint may have a lifetime of months at Io or more (see below).

A second objection to ubiquitous sulfur on Io was formulated by Hapke (1989) and is based on discrepancies between Io's spectra and spectra of S_8 in the 330–420-nm region. Io spectra show less of an abrupt transition at 400 nm than those of S_8 and many other allotropes. Hapke's alternative model used S_2O and polysulfur oxides (PSO) to explain the shape in this wavelength region and these compounds, with SO_2, produced good fits. Moses and Nash (1991) found that spectral matches – with metastable but long-lived sulfur allotropes – were as good or better than those using S_2O and PSO. Therefore, sulfur, even in large amounts, is not precluded and may be preferred as a dominant surface material on Io.

High spectral resolution (1.8-nm) measurements of Io's leading and trailing hemispheres from HST by Spencer *et al.* (1995) were compared with models containing SO_2+sulfur (from Moses and Nash, 1991) and PSO + SO_2+ S_2 (from Hapke, 1989). Excellent fits were found for each set of candidate species although the 560-nm band is somewhat discrepant. Nash (1993) suggested that $Na_2S + S_2O$ provided a better fit in this wavelength region. S_2O samples show an absorption band at 560 nm but this is probably due to S_4 in the laboratory samples (Hapke, 1989). Inclusion of S_4 absorption in the models considered by Spencer *et al.* may improve the fits without resorting to sodium sulfide or disulfur monoxide.

Io's 560-nm feature was first observed by Johnson and McCord (1970) and is a persistent feature. If it is attributed to S_4, and if S_4 is unstable on Io, the global occurrence and persistence of the feature suggests continuing production of S_4. Sources may include ultraviolet photolysis or radiolysis by energetic electrons and ions from Jupiter's magnetosphere, as well as continual replacement by plume S_4 and

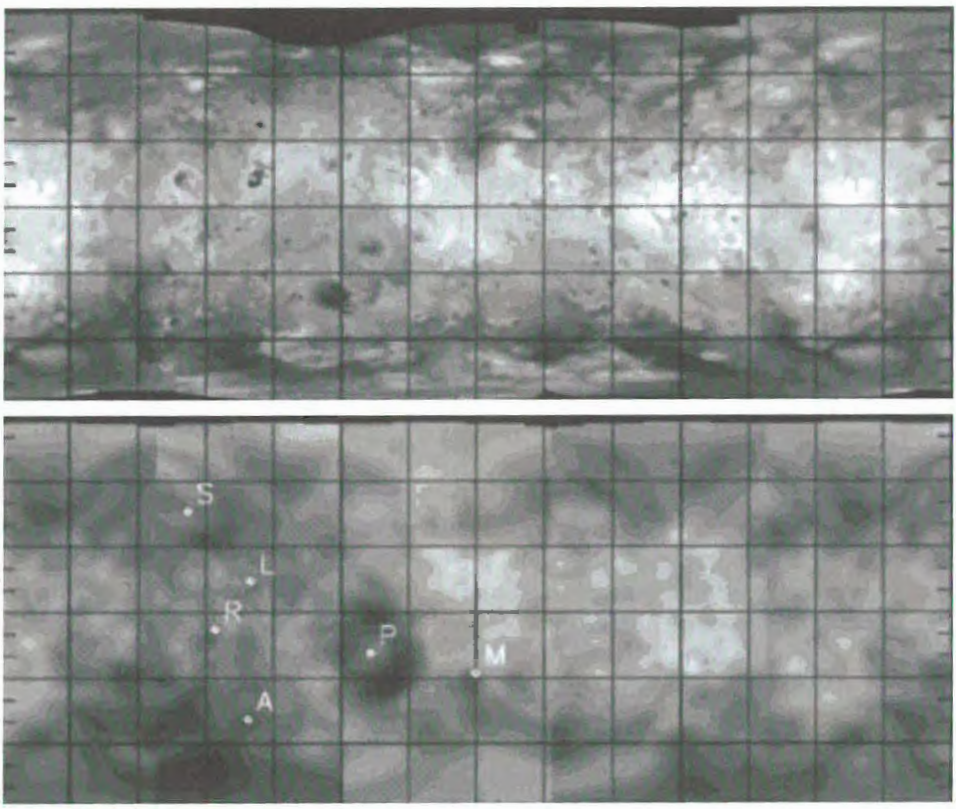

Figure 9.5. Map of Io's S_4 feature. Absorption by tetrasulfur, shown in the bottom panel as black, is evident in Pele's (P) deposition ring and polar regions. A reference map is at the top (from Spencer *et al.*, 1997).

S_2 (direct deposition of S_2 and annealing of S_2 deposits form S_4) and perhaps S_2O (partial thermal decomposition of S_2O form S_3 and S_4 (Hapke, 1989; Hapke and Graham, 1989)).

Evidence for plume sources of S_4 or S_4 precursors is given in HST images indicative of the absorption strength in the 560-nm band (Spencer *et al.*, 1997). These images show strong red absorption in the Pele deposition ring and the polar regions (Figure 9.5). Gaseous species present in Pele-like plumes include SO_2, S_2, SO, and S (Zolotov and Fegley, 2000). The computed molar concentration of disulfur monoxide is about 1/1,000 that of SO_2 and S_2. S_3 and S_4 are even less abundant than S_2O. Thus, Spencer *et al.* (2000) and Zolotov and Fegley (2000) concluded that photolyzed S_2 deposited by the plume could produce S_3 and S_4 in the ring and that this source was more likely that one involving S_2O. Many red regions on Io have faded to the background yellow over time. The lifetime of S_4, if that is the chromophore, is difficult to estimate for Pele due to its continual activity, but a red, Pele-sized ring south of Karei disappeared 2 months after its initial observation (Geissler *et al.*, 2004).

The Pele plume's O/S ratio in 1999 was about 1.5 (Zolotov and Fegley, 2000) but the gas signature of the Pele plume is variable with time. Additional plumes containing S_2 have been inferred (Jessup *et al.*, 2005). Using Douté *et al.*'s (2001) SO_2 map and assuming that the non-SO_2 material is S_8, then elemental sulfur is slightly more abundant by area than SO_2 in the equatorial region (area ratio $\sim 0.6:0.4$) and the average equatorial oxygen to sulfur ratio is $O/S \sim 0.5$. However, the temporally variable fractionation and an unknown gas-to-particulate ratio preclude any quantitative comparison between the relative abundance of SO_2 and S_8 in plumes and deposits on the surface.

The red color of the poles resembles red sulfur glass and it was suggested that this form, possibly produced by radiolysis, would be more stable at the colder poles than in lower latitudes (Spencer *et al.*, 1997). Wong and Johnson (1996b) suggested that SO_2 condensing at the poles would be quickly radiolyzed and continually produce a dark sulfurous residue. The poles are covered by SO_2, yet are dark in the visible, so the SO_2 frost layer must be quite thin and radiolysis must be more rapid than the condensation rate ($\sim 10^{12}$ SO_2 molecules cm^{-2} s^{-1}). Wong and Johnson find that each molecule has received ~ 10 eV which is sufficient to decompose SO_2 and produce dark refractory material.

A possible sulfur feature is found in the broad absorption extending from 1 μm (or less) to about 1.6 μm (Figure 9.1). It was first noted by Pollack *et al.* (1978) and confirmed by *Galileo* measurements (Carlson *et al.*, 1997). The absorption appears to be pervasive on Io although it is absent in Pele's deposition ring and diminished in some dark regions including the green deposits within the Cbaac caldera (Lopes *et al.*, 2001). The absorption is strongest in the southern polar region. This absorption has been attributed to long-chain sulfur polymers by Carlson (2002), based on spectral similarities to radiation products formed in proton irradiation of sulfates (Nash and Fanale, 1977). This long-wavelength absorption feature may be due to sulfur dangling bonds (Eckert and Steudal, 2003; Hosokawa *et al.*, 1994). Other suggested identifications, discussed later, include iron-containing salts or feldspars (Pollack *et al.*, 1978) and iron sulfide (FeS_2, "fools gold", Kargel *et al.*, 1999).

Though not diagnostic of specific substances, the wavelength and slope shift of the visible absorption edge of Io can be attributed to the general types of impurities common in terrestrial volcanogenic sulfur (Kargel *et al.*, 1999; Kargel *et al.*, 2000; MacIntyre *et al.*, 2000); these spectroscopic effects are somewhat like some of those induced by radiolysis and can similarly produce various colored forms of sulfur. An example is the reddening modification due to dissolution of Te in sulfur (Figures 9.2 and 9.3); similar effects have been shown for Se-doped sulfur (Kargel *et al.*, 2000; MacIntyre *et al.*, 2000). This similarity can be understood because both mechanisms involve breaking of sulfur polymer bonds. Since we know that radiolysis occurs, and chemical impurities are inevitable, probably both mechanisms contribute to the color palette of Io. Other elements, such as phosphorus, cause tangling of sulfur polymer bonds, thereby inducing a different set of physical effects on sulfur; in large amounts, phosphorus forms a series of brightly colored yellow and red phosphorus sulfides. All of these elements affect the viscosity of molten sulfur and its freezing behavior, and so they have additional spectroscopic effects related to crystallization vs. quenching and annealing.

9.2.3 Sulfur dioxide

Properties of sulfur dioxide

Physical properties. SO_2 is a colorless gas at room temperature, for low-pressure liquefying at ~263 K and freezing at ~200 K. Over the temperature range from 90 K and 120 K which represents approximate extremes for non-volcanic areas on Io, the SO_2 vapor pressure varies by five orders of magnitude, from 10^{-4} nbar to 10 nbar. Consequently, there is a diurnal sublimation and condensation cycle, transporting and redistributing SO_2 across the surface. SO_2 is amorphous when condensed at temperatures <70 K, but crystallizes for temperatures >70 K (Schmitt *et al.*, 1994). Condensed SO_2 forms many different textures (Nash and Betts, 1995). The condensation, evaporation, and metamorphism of pure SO_2 and mixed ices at temperatures relevant to Io have been discussed by Sandford and Allamandola (1993).

Spectral properties. The fundamental absorption bands of SO_2 occur at 19 μm (520 cm^{-1}), 9 μm (1,140 cm^{-1}), and 7.1–7.7 μm (1,300–1,345 cm^{-1}) for the ν_2, ν_1, and ν_3 vibrations, respectively (see Schmitt *et al.*, 1994; Khanna *et al.*, 1995; Nash and Betts, 1995, for near- and mid-infrared spectroscopic studies). In crystalline materials these vibrations are modified by crystal field effects and also form combination bands with other molecular (internal) modes and lattice phonons (external modes) (Khanna *et al.*, 1995; Quirico *et al.*, 1996). Numerous combination bands produce a rich infrared absorption spectrum in the 1.9–5-μm region; Figure 9.6 shows theoretical reflectance spectra for various grain sizes based on the optical constants measured by Schmitt *et al.* (1994). Infrared reflectance spectra of SO_2 frosts have been measured by Hapke (1979), Smythe *et al.* (1979), Fanale *et al.* (1979), and at higher resolution by Nash and Betts (1995). Far-ultraviolet to near-infrared spectra of frosts were obtained by Hapke *et al.* (1981) and Wagner *et al.* (1987). Visible and near-ultraviolet reflectance spectra were measured by Nash *et al.* (1980). A very sharp edge at 330 nm is found with a reflectance minimum at ~280 nm and a weaker absorption at 350 nm. Hapke *et al.*'s spectra show these bands and other reflectance minima at 225 nm and 184 nm (Wagner *et al.*, 1987). The *Solar System Ices* book (Schmitt *et al.*, 1998a) contains useful reviews of SO_2 properties by both Schmitt *et al.* and Nash and Betts.

Radiolytic properties. Proton bombardment of SO_2 ice produces SO_3 (monomeric and polymeric), sulfur, and sulfate (Moore, 1984). Irradiation of liquid SO_2 with γ-rays (which produce ~500 keV Compton electrons) yields SO_3, S, and O_2, the latter probably produced in $O + SO_3$ reactions (Rothschild, 1964). Similar reactions may occur in the solid phase. SO_2 subjected to electrical discharge produces SO_3, S_2O, S_3, S_4, O_3, and polysulfur oxides (Hopkins *et al.*, 1973).

Spectroscopy and spectral mapping of Io's SO_2

SO_2 was first identified in Io's atmosphere from absorption in the ν_3 band (Pearl *et al.*, 1979). This identification prompted laboratory experiments that quickly explained Io's 4-μm absorption feature (Cruikshank *et al.*, 1978; Pollack *et al.*, 1978; Fink *et al.*,

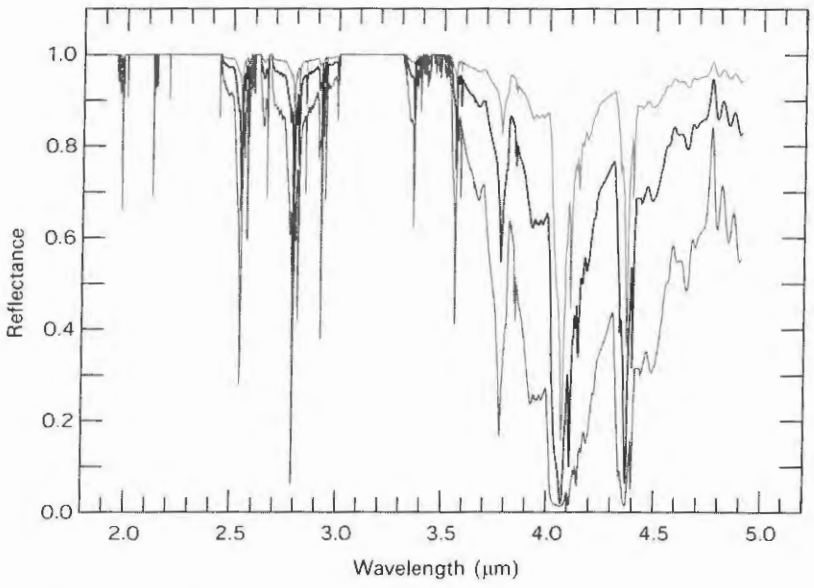

Figure 9.6. Theoretical reflectance spectra for SO_2 frost. The diffuse reflectance spectra of optically thick frosts of 10, 100, and 1,000 μm grains are shown as blue, black, and red lines, respectively (see color section). The optical constants of Schmitt *et al.* (1994, 1998b) were used.

1978) as condensed SO_2 (Hapke, 1979; Fanale *et al.*, 1979; Smythe *et al.*, 1979). Since then, Io's surficial, atmospheric, and extra-atmospheric SO_2 has been mapped and monitored by various techniques.

The surface component is measured at ultraviolet and infrared wavelengths. The sharp ultraviolet edge at 330 nm observed in Nelson and Hapke's (1978) ground-based measurements (Figure 9.1) was originally attributed to sulfur but later found to be consistent with laboratory spectra of SO_2 (Nash *et al.*, 1980). This edge was also found in IUE spectra and these spectra were used to map the longitudinal distribution of SO_2 (Nelson *et al.*, 1980; Nelson *et al.*, 1987), finding that the SO_2 abundance was stable over 8 years. Maximum SO_2 abundance was found in Io's leading hemisphere, particularly in the longitude range of 90–240 W. The SO_2 abundance was minimum in the 300–30 W region.

The 200–310-nm spectrum of Io has recently been obtained from HST and shows both atmospheric and surficial SO_2 (Jessup *et al.*, 2002). There may still be some minor puzzles about Io's UV spectrum. The 225-nm SO_2 absorption found in Hapke *et al.*'s spectrum is not apparent in the HST measurements, and the 350-nm feature appears to be absent. It may be that strong sulfur absorption hides the latter feature. Although sulfur absorption could also influence the 200- to 300-nm spectrum, SO_2's extreme volatility probably produces a thin, ultraviolet-opaque frosting over any exposed, cold sulfur.

Ground-based infrared measurements by Howell *et al.* (1984) showed that SO_2 occurred as a frost, rather than an adsorbate, and was present in most units on Io's surface, in contrast to earlier ultraviolet analyses that indicated SO_2 covering <20% of the average projected surface area (Nash *et al.*, 1980). Howell *et al.* pointed out that the ultraviolet and infrared results were consistent if analyzed using intimate mixing rather than areal mixing as used in the earlier ultraviolet study.

Other spectral measurements of Io's SO_2 were performed by Cruikshank (see Salama *et al.*, 1994), Howell *et al.* (1989), Trafton *et al.* (1991), Larson *et al.* (1992), Lester *et al.* (1992), Salama *et al.* (1994), Sandford *et al.* (1994), and Schmitt *et al.* (1994). Many of the features observed in the spectra were misidentified (see later discussions) due to the lack of laboratory SO_2 spectra, a situation rectified by the laboratory work of Schmitt *et al.* (1994) and Nash and Betts (1995). Of particular note are two weak SO_2 lines observed from Io (at 1.982 and 2.125 μm) that required centimeter path lengths to observe in the laboratory. Sandford and Allamandola (1993) inferred that some of Io's SO_2 is present as a glassy, transparent, and relatively thick ice and not as a frost, consistent with rapid annealing of surface deposits. Multiple refractive scatterings through large grains is also a possibility. Using NIMS data and recently developed analysis algorithms, Soderblom *et al.* (in preparation) have mapped the strength of these weak bands (and others), showing that they appear over most of Io but are strongest in the equatorial regions (Figure 9.7).

A high-resolution spectrum of Io's leading hemisphere has been obtained from the ISO and presented by Schmitt and Rodriguez (2003). Analysis of this spectrum is currently underway.

SO_2 spatial distribution and processes

The *Galileo* NIMS experiment obtained low spatial resolution (120–350 km per pixel) spectral maps on global scales. SO_2 is found everywhere, except in hot volcanic areas (Carlson *et al.*, 1997; Douté *et al.*, 2001). The fractional coverage and mean grain size of SO_2 frost, assumed to be linearly mixed with a spectrally neutral component (e.g., sulfur), has been mapped by Douté *et al.* (2001) using numerous NIMS data sets. These two properties provide clues about the physical state of solid SO_2 which depends on the relative rates of SO_2 condensation, metamorphism, and sublimation (Douté *et al.*, 2001, 2002, 2004). The fractional coverage and mean grain size are combined into a spectral unit map (Douté *et al.*, 2001; Figure 9.8) and can be discussed in terms of four units: I, rich in SO_2 with fine-grained frost; II, rich in SO_2 with coarse-grained frost; III, depleted in SO_2, fine-grained frost; and IV, depleted in SO_2, coarse-grained frost.

A layer of relatively fresh SO_2 frost (Unit I) covers 50–70% of large areas mostly located at medium and high latitudes (30°–60°) and generally devoid of permanent hot spots. At the margins of these areas, the SO_2 coverage remains high but the mean grain size increases substantially, suggesting metamorphism. These SO_2-rich regions show a correlation with active plumes, the plumes generally being on the same meridian but at a lower latitude. One exception is Prometheus, the closest field of abundant SO_2 being to the east, in Bosphorus Regio (100°–150° of longitude).

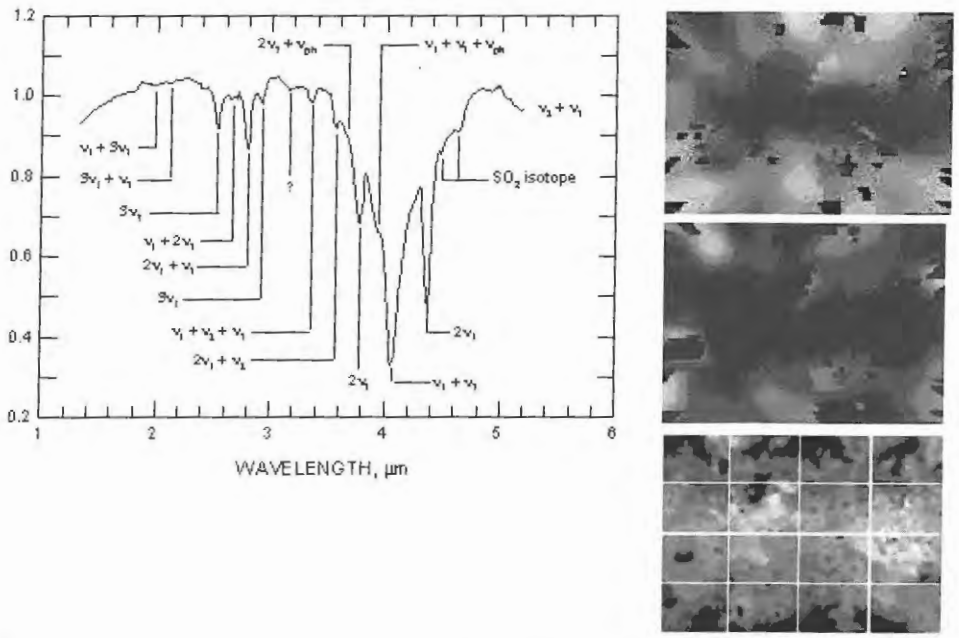

Figure 9.7. Spectrum of Io and equivalent-width maps. Maps of the absorption strength (equivalent width) of the 1.98-μm SO_2 band (*top*) and the 3.15-μm band (*middle*) are shown at the right, with black signifying more absorption. Note the strong equatorial enhancement of the unknown 3.15-μm absorber (possibly H_2O) and its correlation with both the weak, long-path-length SO_2 feature and the bright deposits in the Io reference map (*bottom*). (See also color section.)

Nonetheless all these regions likely represent condensation areas of SO_2 gas migrating from the plumes. The plumes consist of gas and particles that rise to altitudes of tens to hundreds of kilometers before collapsing back and striking the surface at supersonic speeds, generating shock waves and high pressures (Zhang *et al.*, 2003). The pressure increase causes partial dynamic condensation of SO_2, often forming rings of fallout material. The remaining gas contributes to a net longitudinal flux of volcanic SO_2 that flows toward medium and high latitudes (Douté *et al.*, 2001, 2002; Moreno *et al.*, 1991; Wong and Johnson, 1996a, 1996b). The gas condenses where the average temperatures are sufficiently low (~110 K).

For a given condensation field associated with a plume, the degree of metamorphism will depend on the condensation rate compared with the metamorphism timescale. The green (Unit I) regions associated with Pele–Pillan, Marduk, Amirani–Maui, and Prometheus may exhibit the most recent activity and the highest SO_2 emission rate. Culann, Volund, and Zamama appear to be less active.

The regions depleted in SO_2 (SO_2 surface coverage <35%, Units III and IV) represent approximately 60% of the total surface area observed by NIMS. The Jupiter-facing quadrant of the trailing hemisphere contains many of these

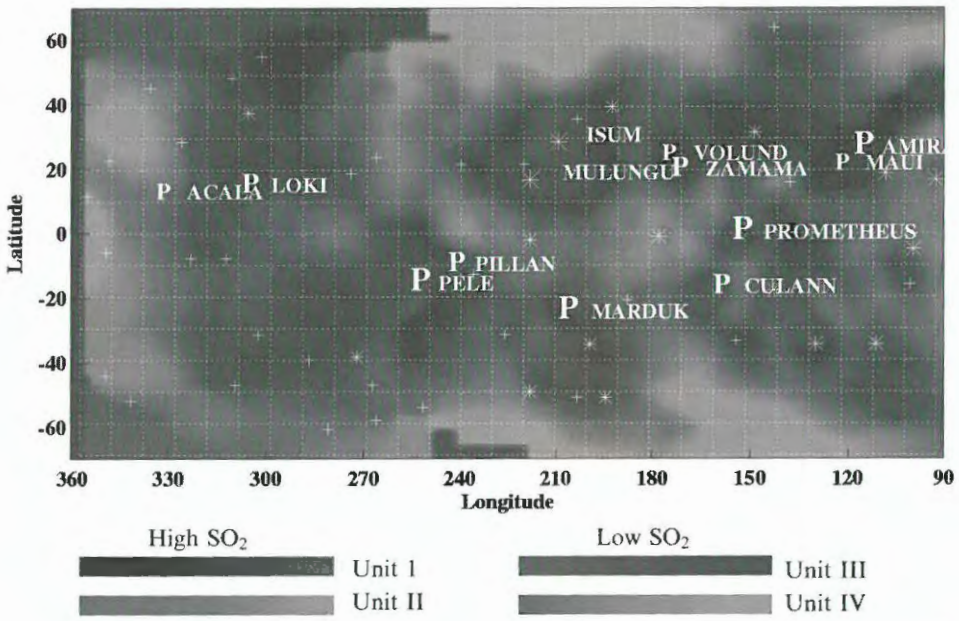

Figure 9.8. Sulfur dioxide spectral unit map. The plumes (P) are sources of fine-grained SO_2 frost (Unit I, green; see color section) deposits, generally poleward of the low-latitude plumes. Hot spot locations are denoted with stars and crosses, with stars being long-lived hot spots and crosses denoting sporadic thermal features. Metamorphosed SO_2 snowfields (Unit II) are shown as light green and yellow. SO_2-poor areas (Units III, IV) occur in the 270 to >360°W longitude region.

SO_2-poor regions, a finding consistent with Nelson *et al.*'s (1980, 1987) measurements of the longitudinal distribution of SO_2, noted previously. The SO_2-frost depleted regions contain many hot spots and plumes. Recent deposition of hot pyroclastic flow materials from nearby volcanic centers and/or mean temperatures above the stability point of SO_2 in the range ≈110–200 K (Douté *et al.*, 2002) may prevent the formation of significant frost deposits. Isum and Mulungu are hot spots centered within an extended area displaying remarkably low SO_2 frost coverage. These hot spots lack plumes to provide SO_2 and the regions may also possess higher mean temperatures than elsewhere, resulting in low SO_2 coverage. Marduk and Zamama, in contrast, are located in regions showing high SO_2 abundance. This suggests that the condensation/sublimation ratio is above the average of these thermally active regions. A higher SO_2 production rate and/or lower regional temperatures could provide an explanation.

Optically thick but patchy frost deposits lie near the equator of the anti-Jovian hemisphere and are characterized by medium frost coverage (35–50%) and by coarse grains (300–500 μm), as indicated in the 1.98-μm map discussed above (Figure 9.7). The condensation of volcanic SO_2 can occur during night-time, but under sunlight equatorial frost sublimates. The sublimational atmosphere creates a high-pressure zone that prevents gaseous SO_2 from spreading from the plumes to the equator. Io's

equatorial temperatures are often close to the SO_2 instability point, favoring metamorphism of the frost and perhaps distillation of SO_2 by repeated sublimation and condensation. Some equatorial regions (e.g., Bosphorus Regio) display an SO_2 areal abundance that exceeds the usual background level of 45% (Douté *et al.*, 2002). This enhanced concentration may be due to either an intense incoming flux of gas coming from a neighboring plume (dynamic condensation) or a negative thermal anomaly (~110 K) causing cold trapping.

Mechanisms controlling the emission of SO_2 and other compounds from different types of volcanoes, and how these products evolve, can be derived from regional-scale observations at high spatial resolution (Douté *et al.*, 2002; Douté and Schmitt, 2003; Lopes-Gautier *et al.*, 2000; Lopes *et al.*, 2004; Williams *et al.*, 2002). Persistent hot spots such as Prometheus, Culann, Surya, and Tupan are thought to emit a great variety of gases, some of which will condense at Io's surface near their source regions. Associated fields of freshly condensed SO_2 are easily observed, and deposits of more refractory compounds with higher (e.g., S_8) or lower (e.g., NaCl) molecular weight may also be present (although their exact nature is unknown). Three different mechanisms of emission are proposed for the volatile compounds, and supported by the distribution maps. These are (a) the interaction between flowing lava and pre-existing volatile deposits on the surface, (b) the direct degassing from the lava, and (c) the eruption of a liquid aquifer from underground.

The geometric elongation of Prometheus's SO_2 deposition ring coupled with higher SO_2 concentration values within its eastern part is the best illustration of mechanism (a). Temporal development of a 95 km long lava field displaced the sublimation front, and thus also the plume and its associated circular ring of deposition.

Amirani also emits a large amount of SO_2 gas, perhaps by a similar interaction of fresh lava with the volatiles of the underlying plains. Nevertheless, SO_2 frost is not the major component of the bright white ring surrounding Amirani and seen in visible images. The eruption style is presumably different with the white compounds being degassed from the lava at a single vent (mechanism (b)) and SO_2 being principally sublimated along the numerous active boundaries of the Amirani flow (mechanism (a)). Mechanism (b) may operate for some Pillanian eruptions like the Thor eruption that occurred during the summer of 2001 (Lopes *et al.*, 2004) and that created a 800 km diameter white ring of fallout partly composed of solid SO_2.

Mechanism (c) may have been operative inside a small caldera to the east of Chaac and on the north-western flank of the volcanic edifice Emakong. These areas exhibit an extremely deep SO_2 absorption that is indicative of abundant, pure, and perhaps icy SO_2 deposits. The SO_2 is topographically confined by the caldera walls, suggesting sapping or an eruption of an SO_2 liquid aquifer (Smythe *et al.*, 2000, Lopes *et al.*, 2001).

9.2.4 Other sulfoxides

Sulfur monoxide

We mention SO for completeness since it is an atmospheric constituent but is not observed as a surface component. Lellouch *et al.* (1996) found SO in the atmosphere at

a level of a few % of SO_2 and SO^+ was found in Io's ionosphere (Russell and Kivelson, 2001). SO can be produced photochemically in the atmosphere and is an important component in plumes, second only to SO_2 (Zolotov and Fegley, 1998, 2000). Indeed, SO infrared electronic-band emission has been observed during eclipse and attributed to thermally excited SO in plumes (de Pater *et al.*, 2002) see also (McGrath *et al.*, 2004).

The vapor pressure and condensation properties are not established; we assume that SO molecules can condense or be trapped on Io's surface. Sulfur monoxide is a reactive, unstable compound, decomposing to form SO_2 and S_2O (Baklouti *et al.*, 2004). The fundamental vibrational transition in the condensed phase at 31 K is at 1,137 cm^{-1} (Hopkins and Brown, 1975) so the overtone band will occur at ~4.4 μm but the exact position is not established. Strong overlapping sulfur dioxide absorption features occur in this region in Io's spectra; consequently, searches for the presence of SO will be hindered by imprecise knowledge of the SO band position.

Sulfur trioxide

Sulfur trioxide and sulfur are the primary products of SO_2 radiolysis (Moore, 1984; Rothschild, 1964). SO_3 molecules that accumulate are themselves destroyed by radiolysis, producing SO_2 and the secondary product O_2 that can escape the surface. With time, an initial SO_2 surface would be transformed to elemental sulfur and atmospheric oxygen if there are no other processes affecting the sample. This mechanism, if operative over a long period of time, potentially could explain the elemental sulfur-rich surface of Io as an additional process or an alternative to the internally driven process described by Lewis (1982), which could yield elemental sulfur by incongruent melting of metal sulfides. During this slow degradation process, a radiolytic equilibrium will be attained, with a constant $SO_3 : SO_2$ abundance ratio. Radiolysis by electrons at Io will produce $\sim 3 \times 10^{12}$ SO_3 molecules s^{-1} cm^{-2} and an $SO_3 : SO_2$ ratio of 0.1 (or greater) may be expected, based on results by Moore. However, two processes will reduce the $SO_3 : SO_2$ ratio. The first is resurfacing and was considered earlier by Moore for proton excitation, predicting an $SO_3 : SO_2$ ratio of 10^{-4}. This ratio will he different for electron irradiation. A resurfacing rate of 1 mm yr^{-1} provides $\sim 6 \times 10^{13}$ molecules s^{-1} cm^{-2}, a factor of 20 greater than the SO_3 production rate by electron irradiation on Io, implying an $SO_3 : SO_2$ ratio of 0.05. The second limiting effect is sublimation and condensation, occurring at a rate of $\sim 0.4 \times 10^{14}$ SO_2 molecules s^{-1} cm^{-2}, a factor of 13–130 times greater than the SO_3 production rate. Any SO_2 lost by radiolysis is quickly replenished, gradually burying the SO_3. We therefore do not expect SO_3 to be present as a major species but it may be present at the few % level.

Khanna *et al.* (1995) studied the spectra of SO_3 at temperatures relevant to Io and found absorption features at 465 and 524 cm^{-1} that they suggested may be present in Io's thermal emission spectrum (see spectral locations, Figure 9.4). The two corresponding bands in the *Voyager* IRIS spectrum were attributed to S_8 and SO_2 by Pearl (1988) and Hanel *et al.* (2003) but the natural strength of the sulfur band is 100 times weaker than that of the SO_2 band. Therefore, if the abundances of sulfur and

SO_2 were comparable on Io's surface then some other absorber produces the 465 cm^{-1} emissivity feature. Khanna *et al.* suggest that SO_3 contributes to both features.

Laboratory spectra also show an SO_3 absorption band complex with prominent features at 4.04 and 4.09 μm (Khanna *et al.*, 1995). These bands straddle the 4.07 μm SO_2 feature but NIMS Io spectra do not show any characteristics attributable to SO_3 absorption (Schmitt and Rodriguez, 2003). Quantitative upper limits have not been established. The most likely locations for SO_3 to be present are the trailing hemisphere and polar regions.

Disulfur monoxide and polysulfur oxides

Disulfur monoxide (S_2O, arranged as bent SSO) is an unstable molecule at Io temperatures, decomposing to form SO_2 and S_3 (Steudel and Steudel, 2004). S_3 and S_2O can then react to form S_5O and bimolecular decomposition of the latter produces SO_2, S_3, and S_4. This decomposition of S_2O occurs at 100 K or below (Blukis and Myers, 1965; Hapke and Graham, 1989) and explains the red color of S_2O when deposited at cryogenic temperatures (Steudel and Steudel, 2004). Pure or nearly pure S_2O concentrations can undergo radical-chain polymerization forming polysulfur oxides (PSO) – chains of sulfur atoms with occasional oxygen atoms attached to the side.

The fundamental SO stretch band of pure condensed S_2O occurs at 1,165 cm^{-1}, the SO bend at 388 cm^{-1}, and the SS stretch at 679 cm^{-1} (Blukis and Myers, 1965). The SO stretch bands for S_5O and PSO are at 1,119 and 1,123 cm^{-1}, respectively (Steudel, 2003c). The formation and mid- to near-infrared spectra of S_2O and PSO are currently being studied in B. Schmitt's laboratory (Baklouti *et al.*, 2004). Photolysis of S_2O produces a cyclic isomer (Lo *et al.*, 2002).

The original motivation for Hapke's (1989) suggestion for S_2O and PSO on Io was to explain Io's near-ultraviolet reflectance spectrum that he showed was discrepant with $S_8(\alpha)$ reflectance. It was later shown that reflectance by other sulfur allotropes was consistent with Io's spectrum (see above), so there is presently no need to invoke S_2O or PSO on Io. Additionally, S_2O is a minor constituent in the plumes (<1% molar, Zolotov and Fegley, 2000) and will be reduced even further by thermal decomposition reactions as discussed above, producing plume S_5O that will be deposited on the surface and then photolyzed to SO_2 and elemental sulfur (Steudel and Steudel, 2004). Conversely, plume sulfur monoxide (see above) may react to form S_2O, so the monomers and PSO may be present as minor species with their signatures evident as overtones at ~2,330 cm^{-1} (4.29 μm) and 2,246 cm^{-1} (4.45 μm) respectively. These predicted positions straddle the strong $2\nu_1$ band of SO_2 and although no features attributable to S_2O or PSO are evident, uncertainty in the positions and strengths preclude establishing upper limits. The cyclic form of S_2O may be present on Io based on features at 800 and 580 cm^{-1} in the *Voyager* thermal emission spectrum that may match transitions of cyclic S_2O (Lo *et al.*, 2002).

Sulfates, sulfites, sulfuric acid, and sulfurous acid

The most oxidized form of sulfur is sulfate, SO_4^{2-}. This chemical class is a common and stable end-product of sulfur oxidation. Sulfite, SO_3^{2-}, is a less oxidized group.

Numerous sulfate and sulfite salts have been studied and suggested as candidates for Io's surface (Nash and Fanale, 1977) and could be observable through combination bands in the 4–5-μm region (Nyquist *et al.*, 1997). There are no obvious unidentified features in NIMS Io spectra in this region (a band at 4.62 μm thought possibly due to a sulfate is here attributed to SO_2). Alkali sulfates are minor species in Io plumes but can form localized deposits (see the Na_2S discussion below). Upper limits for sodium sulfate and sulfite on Io have been established at 25% and 40%, respectively, by Howell *et al.* (1989). The NIMS data can provide more stringent upper limits for these and other salts but this work has not yet been performed.

Sulfuric acid, H_2SO_4, a familiar substance in the laboratory and in industry, is common in acid fumaroles and hot springs on Earth and is likely also on Europa and on Mars, where ice and water vapor indicate a fairly high activity of H_2O. Sulfuric acid is not stable where water activity is nil, and this would appear to describe Io.

In contrast to many acids (e.g., sulfuric, carbonic, and hydrochloric) the undissociated sulfurous acid molecule H_2SO_3 has never been observed in the laboratory or nature. Voegele *et al.* (2004) have calculated the thermodynamic stability of this molecule at low temperatures, finding that it is long-lived at 100 K and suggested that proton irradiation of Io's SO_2 surface would produce H_2SO_3. However, using the proton flux of $6.5 \times 10^4\ s^{-1}\ cm^{-2}$ from Paranicas *et al.* (2003), the production rate of H_2SO_3 molecules would be at most $3.25 \times 10^4\ s^{-1}\ cm^{-2}$. This rate is only one billionth of the mean resurfacing rate (see the SO_3 section), so it is highly unlikely that sulfurous acid is present in measurable quantities.

9.2.5 Sulfides

Hydrogen sulfide, H_2S, has been often suggested as a surface component on Io based on features at 3.9 μm in spectra of Io (Nash and Nelson, 1979; Nash and Howell, 1989; Salama *et al.*, 1990). However, SO_2 exhibits a shoulder at this wavelength and *Galileo* NIMS spectra are consistent with SO_2 absorption alone over most of Io. A few isolated regions show enhanced absorption at 3.92 μm that is inconsistent with SO_2. Schmitt and Rodriguez (2003) performed laboratory studies of H_2S and compared their results with NIMS spectra. Dilute H_2S mixed in SO_2 does not fit the NIMS spectra as the H_2S band is at ~3.85 μm; an upper limit of 10^{-4} is given for the dilute H_2S mixing ratio (Schmitt and Rodriguez, 2003). Grains of H_2S ice do absorb at 3.92 μm but H_2S ice is very unstable at Io temperatures, with a vapor pressure 10^4 times that of SO_2 at 110 K. Since H_2S is not observed in the atmosphere (McGrath *et al.*, 2004) it seems unlikely that H_2S ice is abundant on the surface. We note however that during the I27 orbital pass of Io by *Galileo*, Russell and Kivelson (2001) found a broad ion cyclotron signature in the vicinity of H_2S^+, Cl^+, and S^+ ions. These signals were absent on other orbits and if the I27 signals are indeed due to H_2S, sulfur, and chlorine ions, then the enhancement may be caused by time variability of Io's exosphere that may in turn be related to transient volcanic emissions.

H_2S_2 has been considered by Schmitt and Rodriguez (2003) who point out that the abundance of this species in Io plumes should be lower than the HS abundance and should vary as the H/S ratio. Though the position of the SH stretching mode of H_2S_2

diluted in SO_2 is not known it may occur at 3.92 μm. For H_2S_2 to be abundant enough to produce the observed 3.92 band (see the Cl_2SO_2 discussion), it would require higher H/S ratios than are consistent with global limits and would result in the production of H_2S and H_2O at levels that are not observed.

Sodium sulfide, Na_2S, has also been a popular candidate for Io's surface as this molecule contains sodium, known to be in the Io torus, as well as sulfur. It was originally proposed by Nash and Nelson (1979) who found a 4-μm feature in spectra of Na_2S that might have explained Io's feature, but the laboratory 4-μm feature was later found to be due to carbonate contamination (Nash, 1988). In the visible region, Na_2S exhibits an absorption feature at ~560 nm (see S_2 above) and mixtures of the sulfide with sulfur and SO_2 produce good fits to Io's spectrum (Nash, 1993). He suggested sulfide volcanism and that Na_2S deposits could cover 15–20% of Io's surface. Na_2S is only a minor component in Io plumes (Fegley and Zolotov, 2000; Moses *et al.*, 2002; Schaefer and Fegley, 2005), even for those with low Cl : Na ratios, and an average molar abundance is estimated at $<10^{-4}$. However, as with Na_2SO_4 and alkali halides, Na_2S condenses at high temperature and can form localized red deposits around vents and can coat pyroclastic silicate particles (Fegley and Zolotov, 2000). The infrared spectrum of Na_2S appears bland (Nash, 1988) so no identifications or limits are available.

Since Io may have a core containing iron sulfide, it is reasonable to consider the presence of iron sulfides such as FeS_2 (pyrite and marcasite) and FeS (pyrohotite, actually $Fe_{1-x}S$, due to an iron-deficient lattice) (Lewis, 1982). Spectra of these materials, especially pyrite, show considerable variations, but there is generally a broad absorption band extending from the visible to ~1.5 μm with a minimum at ~0.9 μm. Kargel *et al.* (1999) have suggested FeS_2 as a candidate for Io based on the 1-μm band and the colors that FeS_2 imparts to sulfur, being gray–black and green and similar to some colors on Io (see Figure 9.2), and based on the common dispersion of significant pyrite (commonly the major impurity) in terrestrial volcanogenic sulfur. The distribution of the 1-μm absorber on Io may provide clues to whether it is iron sulfide or not. Although the absorber appears to be present over most of Io, and enhanced in the southern polar region, it is deficient in the Pele deposition ring (Carlson *et al.*, 1997). Thus, volcanic plumes appear not to be sources of iron sulfide if this one example is representative. The identity of the 1-μm absorber and the role of iron sulfides is not resolved. Granahan (2004) claimed detection of iron sulfide based on a 3-μm feature. However, the reference sulfide laboratory spectra contained the ubiquitous H_2O 3-μm band (Salisbury *et al.*, 1991) and therefore were not representative of anhydrous iron sulfides.

9.2.6 Metals, salts, and halogen compounds

The discovery of Na and K in the Io neutral torus fostered many laboratory, theoretical, and observational studies of potential Ionian alkali salts and sulfides. A corresponding molecular ion (NaX^+) has been postulated to provide energetic Na atoms in the neutral torus by dissociative recombination (see summary in Thomas *et al.*, 2004a) but the major anion was unknown until Kuppers and Schneider (2000)

discovered Cl^+ in the Io torus, suggesting NaCl as a major salt on Io. Thermochemical models of Ionian plumes with alkali and halogen atoms predicted that NaCl would be the major salt component (Fegley and Zolotov, 2000; Moses *et al.*, 2002; Schaefer and Fegley, 2005).

Sodium chloride and possibly potassium chloride in Io's atmosphere was discovered by Lellouch *et al.* (2003), finally resolving the 28 year old puzzle of the source of Na in the Io torus (Hunten, 2003). Lellouch *et al.* simultaneously measured two NaCl lines and several SO_2 lines so an abundance ratio can be derived although the resulting value is model dependent. Their preferred model is a patchy distribution arising from volcanic sources, with plume SO_2 bouncing once before depositing on the surface while the less volatile NaCl molecules deposit immediately when striking the surface (no bounces). In this model the $NaCl/SO_2$ molar ratio is 0.3–1.3%. The observed $NaCl/SO_2$ ratio is less than the 4% ratio predicted by Fegley and Zolotov (2000) but is consistent with CI chondritic compositions. Volcanic NaCl can deposit on the surface and can be photodissociated, producing atmospheric Na and Cl atoms (Feaga *et al.*, 2004). The NaCl source rate found by Lellouch *et al.* is sufficient to supply the torus. An NaCl surface abundance in the per cent range or less, relative to SO_2, is therefore expected. Surficial NaCl will be hard to observe because rotational transitions are hindered in the condensed state and the fundamental stretch band occurs at 20 μm. NaCl spectra are featureless from the infrared to the ultraviolet. Color centers produced by irradiation have been discussed but are too broad to be diagnostic (see references and discussion in Moses *et al.*, 2002). Since NaCl is not by itself volatile at Io's surface temperatures, there may be a tendency for it to become covered by more volatile materials and thus to get buried.

Another chlorine compound, Cl_2SO_2 (sulfuryl chloride) has been investigated by Schmitt and Rodriguez (2003) who studied the infrared spectrum and vapor pressure of this molecule. They found absorption bands in the NIMS range at 3.92, 3.57, and 4.24 μm. A feature at 3.92 μm is present in localized regions near Marduk that they suggest is possibly due to Cl_2SO_2 produced by reactions of plume-derived atomic chlorine with surface SO_2. Such reactions are observed when Cl_2 is photolyzed in frozen Cl_2–SO_2 mixtures in rare gas matrices and proceeds through the intermediate $ClSO_2$ molecule (see discussion and references in Schmitt and Rodriguez (2003) and Moses *et al.* (2002)). Condensed Cl_2SO_2 has a lower vapor pressure than SO_2 so it is thermodynamically stable on the surface. The unshielded photochemical lifetime is about 3 years and can be greatly increased if minor amounts of sulfur are mixed in. Schmitt and Rodriguez (2003) suggest that a chlorine-rich volcanic eruption at Marduk produced atomic chlorine that then reacted with the surface to produce an ephemeral layer of Cl_2SO_2-rich SO_2. A 1 mm thick layer containing 1% Cl_2SO_2 provides sufficient absorption at 3.92 μm to match the Marduk spectra while the 3.57 and 4.24-μm features are muted, consistent with the observations.

Since chlorine atoms are globally present in Io's atmosphere, $ClSO_2$ and Cl_2SO_2 are continuously being produced (and photochemically destroyed), giving a equilibrium concentration that is less than that observed at Marduk. It is possible that diluted Cl_2SO_2 may explain the emission feature observed by *Voyager* around 587 cm^{-1} (Schmitt and Rodriguez, 2000).

Cl_2S (sulfur dichloride) is predicted to be present in volcanic plumes and is the dominant sulfur–chlorine molecule produced photochemically (Moses *et al.*, 2002). It is dark red in the liquid phase, prompting Schmitt and Rodriguez (2003) to suggest that this molecule may provide the red coloration near Marduk, where the above-mentioned Cl_2SO_2 may have been observed, and possibly elsewhere.

Hydrochloric acid, HCl, may be produced in Io's volcanoes and is the second most abundant hydrogen-bearing volcanic effluent at low H/S atomic ratios, SH being slightly more abundant (Fegley and Zolotov, 2000). The fundamental vibrational mode for the free HCl molecule occurs at about 3.3 μm. The position for trace amounts of HCl in SO_2 ice is not known but may be shifted sufficiently to be a candidate for Io's 3.15-μm absorber.

9.2.7 Water and hydroxides

Water

Early spectroscopic investigations of water on Io were compromised by lack of long path length SO_2 spectra and the inability to simulate Io's rich spectrum in thin film mixture studies. However, despite some earlier mis-steps, all of these studies included a common band that remains unidentified and may be indicative of water or hydroxyl on Io. This suggestive band occurs at 3.15 μm and was first reported by Salama *et al.* (1990) who also reported a companion band at 2.97 μm. They performed laboratory measurements of $H_2O : H_2S : SO_2$ thin films and found features at approximately 2.97 and 3.15 μm. These they attributed to the symmetric and anti-symmetric OH stretch transitions (ν_1 and ν_3) of water dimers and higher multimers complexed with sulfur dioxide $(H_2O)_n \cdot SO_2$. (The bands of monomer complexes occur at shorter wavelengths and are obscured by stronger SO_2 bands in Io's spectrum.) Although the ν_1 transition is much weaker than the ν_3 transition in the free molecule, in H_2O–SO_2 complexes the strengths of the two bands are comparable (Schriver *et al.*, 1988). The 3.15-μm band was also present in Io spectra reported by Sandford *et al.* (1994) but the 2.97-μm feature was absent. The presence of the 3.15-μm band and the absence of the 2.97-μm band was confirmed by both *Galileo* NIMS and ISO measurements (Carlson *et al.*, 1997; Schmitt and Rodriguez, 2003). The near-equality of the ν_1 and ν_3 water complex transitions in laboratory spectra (Schriver *et al.*, 1988) indicates that two bands should be present, and if the measurements of Salama *et al.* (1990) are correct, then a 2.97-μm ν_3 band should be present and of equal or somewhat greater strength than the 3.15-μm band. This is not observed in the *Galileo* or ISO data, contraindicating H_2O on Io. Further laboratory work is required before H_2O can be definitely ruled out. In particular, experiments with small amounts of H_2O in pure SO_2 should be performed as Salama *et al.*'s experiments had H_2S at concentrations 10–30× that of H_2O so $(H_2O \cdot H_2S) \cdot SO_2$ complexes may have formed instead of $(H_2O)_n \cdot SO_2$.

Additional but weak evidence for water is given in localized multi-channel spectra obtained by NIMS after the scanning motion of the grating ceased operation in I24 (Douté *et al.*, 2004). These coarse-resolution data (12 points) exhibit a broad, shallow band at 3 μm that may be indicative of water or a hydrate in localized bright deposits

north-west of Gish Bar Patera. This same band was found by Granahan (2004) in Io's mountainous areas.

Hydroxides

The 3.15-μm feature could arise from the OH stretching transition in a hydroxide. Salama *et al.* (1994) considered NaOH but found a wavelength mismatch. Oxy-hydroxides such as AlOOH (diaspore and boehmite) and FeOOH (goethite) show OH transitions in this wavelength region but none of these provide an exact match. (Riskin, 1974).

9.2.8 Silicates

Formation models of the Galilean satellites predict silicates as a major component, but firm evidence for their presence on the surface is lacking. Silicates may be difficult to detect due to the pervasive SO_2 frosting that covers much of the surface through sublimation and condensation. It is likely that only the warm volcanic regions show exposed silicates; this conjecture is consistent with the low or non-existent concentration of Si in Io's extended atmosphere (Na *et al.*, 1998). A limit of 1.4% of Si relative to Na was found whereas chondritic abundances show Si abundance 22 times greater than that for sodium.

The lack of evidence for silicates is also partly due to the loss, early in the *Galileo* mission, of the NIMS detector that sampled the 1–1.3-μm region that is diagnostic of silicate Fe^{2+} absorption features. This reduced capability was exacerbated by the loss of grating scan motion just as the high spatial resolution portion of the mission began.

While early determinations of the temperatures of Io's volcanoes suggested sulfur volcanism, Carr *et al.* (1979) and Clow and Carr (1980) argued that silicates must be present in the near surface, providing the strength needed to support Io's mountains. Volcanic temperatures of ~900 K observed by Johnson *et al.* (1988) ruled out sulfur volcanism and provided strong evidence for silicate volcanism. *Galileo* measurements indicated even higher lava temperatures, >1,700 K (McEwen *et al.*, 1998), higher than the melting points of common basalts. Such high temperatures require superheating, ceramic volcanism (Kargel *et al.*, 2003), or high melting point silicates (see Chapter 7).

There is suggestive evidence for the presence of Mg-rich, high melting point silicates, in particular for ultramafic rocks called komatiites, magnesium-rich volcanic rocks from the Earth's earliest volcanoes. The SSI camera had filters with average effective wavelengths of 418, 560, 664, 731, 757, 888, and 990 nm for Io (Klaasen *et al.*, 1997). For some of Io's dark calderas a reflectance minimum was found in the 888-nm filter and is suggestive of the presence of a silicate (McEwen *et al.*, 1998; Geissler *et al.*, 1999). Although absorption at this wavelength is often associated with a ferric iron absorption in, for example, hematite, for a few silicate minerals, the usual 1-μm ferrous iron feature of silicates appears at 0.9 μm (see the USGS and ASTER spectral libraries, *http://speclab.cr.usgs.gov* and *http://speclab.jpl.nasa.gov/*, respectively). These minerals are the orthopyroxenes enstatite and hypersthene. Magnesium-rich enstatite is a mineral that has been found in one example of

komatiite – the Commondale greenstone belt of South Africa – although komatiites generally contain the minerals olivine (as does Commondale greenstone) and clinopyroxene. Large amounts of olivine are inconsistent with the SSI data (Geissler *et al.*, 1999) or Pollack *et al.*'s (1978) ground-based spectra. For comparison, some ultramafic rock spectra are presented by Hunt *et al.* (1974).

If high-temperature silicate volcanism has been a frequent or continuous and widespread phenomenon on Io, the possibility exists that volatilization and recondensation of Mg, Fe, Si, and O has caused a significant fractionation of these elements with respect to Ca and Al, with a consequent shift of some silicate magmatic systems outside the region of familiar peridotite-based igneous processes (Kargel *et al.*, 2003). This process can potentially explain an Io that has super-high-temperature silicate magmatism without involvement of iron silicates, since iron-bearing components may have segregated into the core and/or to the base of the mantle under this extreme igneous processing regime. The ceramic volcanism concept involves a reduced importance of Fe–oxide-bearing eutectic igneous phase relations (which characterize normal peridotite- and basalt-based systems) due to the intervention of vapor distillation in the differentiation process. The crust, in this scenario, would be highly enriched in refractory Ca–Al-rich and Fe-poor silicates. Hence, spectroscopists may be looking for the wrong silicate minerals, and the right ones may be hard to detect without having much of an iron component.

The likely presence of highly magnesian orthopyroxene in crustal lava has implications for interior models. In one scenario the mantle and crust, depleted of iron during formation of an iron-rich core, remains undifferentiated by high amounts of partial melting and recycling of the lithosphere back into the mantle (McEwen *et al.*, 1998; Keszthelyi *et al.*, 2004). Alternatively, Io could be strongly differentiated (Keszthelyi and McEwen, 1997), with a low-density felsic crust rich in alkalis and aluminum, a Mg-rich upper mantle (the lava source), and an Fe, Ca-rich lower mantle. Pollack *et al.* (1978) suggested that the 1-μm absorber could indicate the presence of feldspars on Io's surface, consistent with a differentiated crust. However, Keszthelyi *et al.* (2004) argue that orthopyroxene-rich lavas can be present on Io if the crust is continuously mixed back into the mantle.

9.3 SUMMARY

Except for hot volcanic regions, Io's surface is being constantly covered by sulfur dioxide from volcanic plumes. Daily sublimation and condensation of SO_2 frosts the surface, hiding trace plume species. In addition to plume sources, solidified liquid SO_2 flows are also thought to be present on the surface.

The plumes bring other species to the surface. Sulfur is thought to be mainly introduced to the surface as a plume effluent such as S_2, which is converted within the plumes or on the surface to S_4, and then combines to form S_8, sulfur polymers, or both. Minor plume species are NaCl and probably KCl, and atomic chlorine that may produce $ClSO_2$ and related compounds.

If water is present on Io it is rare. A weak, unidentified band at 3.15 μm may indicate the presence of H_2O at the ppm level, but laboratory work needs to establish the spectral position of dilute concentrations of water in SO_2 and sulfur at temperatures relevant to Io. The broad unidentified absorption in the 1-μm region needs to be investigated in order to narrow the range of plausible candidates.

Pyroxene silicates may be present in hot volcanic caldera but the evidence is not conclusive. High spatial resolution adaptive optics near-infrared spectroscopy of volcanic caldera may show the ferrous iron bands of silicates in the 1-μm region. Mid-infrared spectroscopy of volcanic thermal emission may show emissivity features of the emitting surface.

Calculations of the thermo-chemistry of Io's volcanic plumes are important for interpreting observations and predicting species that may be on the surface. Plume spectroscopy is a promising tool to search for new species and improve understanding of this enigmatic satellite.

9.4 REFERENCES

Baklouti, D., B. Schmitt, and O. Brissaud. 2004. Infrared study of lower sulfur oxides on Io's surface. *Bull. Amer. Astron. Soc.*, **36**, 16.07.

Ballester, G. E., M. A. McGrath, D. F. Strobel, X. Zhu, P. D. Feldman, and H. W. Moos. 1994. Detection of the SO_2 atmosphere on Io with the Hubble Space Telescope. *Icarus*, **111**, 2–17.

Bass, A. M. 1963. The optical absorption of sulfur. *J. Chem. Phys.*, **21**, 80–82.

Binder, A. B. and D. P. Cruikshank. 1964. Evidence for an atmosphere on Io. *Icarus*, **3**, 299–305.

Blukis, U. and R. J. Myers. 1965. Disulfur monoxide. III: Its infrared spectrum and thermodynamic functions. *J. Phys. Chem.*, **69**, 1154–1156.

Boring, J. W., Z. Nansheng, D. B. Chrisey, D. J. O'Shaugnessy, J. A. Phipps, and R. E. Johnson. 1985. The production and sputtering of S_2 by keV ion bombardment. In: C. I. Lagerkvist, B. A. Lindblad, H. Lundstedt, and H. Rickman (eds), *Asteroids, Comets, Meteors II*. Uppsala Universitet Press, Uppsala, Sweden, pp. 229–234.

Carlson, R. W. 2002. The diverse surface compositions of the Galilean satellites. In: *Solar System Remote Sensing* (LPI Contribution No. 1129). Lunar and Planetary Institute, Houston, p. 9.

Carlson, R. W., W. D. Smythe, R. M. C. Lopes-Gautier, A. G. Davies, L. W. Kamp, J. A. Mosher, L. A. Soderblom, F. E. Leader, R. Mehlman, R. N. Clark *et al.* 1997. The distribution of sulfur dioxide and other infrared absorbers on the surface of Io. *Geophys. Res. Lett.*, **24**, 2479–2482.

Carr, M. H., H. Masursky, R. G. Strom, and R. J. Terrile. 1979. Volcanic features of Io. *Nature*, **280**, 729–733.

Casal, H. L. and J. C. Scaino. 1985. Transient intermediates in the photochemistry of elemental sulphur in solution. *C. Photochem.*, **30**, 253–257.

Chatelain, Y. A. and J. Buttet. 1965. Electron paramagnetic studies of unstable sulfur forms. In: B. Meyer (ed.), *Elemental Sulfur*. Interscience, New York, pp. 208–215.

Chrisey, D. B., R. E. Johnson, J. W. Boring, and J. A. Phipps. 1988. Ejection of sodium from sodium sulfide by the sputtering of the surface of Io. *Icarus*, **75**, 233–244.

Clow, G. D. and M. H. Carr. 1980. Stability of sulfur slopes on Io. *Icarus*, **44**, 269–279.

Cruikshank, D. P., T. J. Jones, and C. B. Pilcher. 1978. Absorption-bands in spectrum of Io. *Astrophys. J.*, **225**, L89–L92.

de Pater, I., H. G. Roe, J. R. Graham, D. F. Strobel, and P. Bernath. 2002. Detection of the forbidden SO $a^1\Delta$-$X^3\Sigma^-$ rovibronic transition on Io at 1.7 mm. *Icarus*, **156**, 296–301.

Douté, S. and B. Schmitt, 2003. Io's thermal stage and the spatial distribution of solid SO_2 abundance. *Icarus* (submitted).

Douté, S., B. Schmitt, R. Lopes-Gautier, R. Carlson, L. Soderblom, and J. Shirley. 2001. Mapping SO_2 frost on Io by the modeling of NIMS hyperspectral images. *Icarus*, **149**, 107–132.

Douté, S., R. M. C. Lopes, L. W. Kamp, R. W. Carlson, and B. Schmitt. 2002. Dynamics and evolution of SO_2 gas condensation around Prometheus-like volcanic plumes on Io as seen by the near-infrared mapping spectrometer. *Icarus*, **158**, 460–482.

Douté, S., R. Lopes, L. W. Kamp, R. Carlson, and B. Schmitt. 2004. Geology and activity around volcanoes on Io from the analysis of NIMS spectral images. *Icarus*, **169**, 175–196.

Eckert, B. and R. Steudal, 2003. Molecular spectra of sulfur molecules and solid sulfur allotropes. *Top. Curr. Chem.*, **231**, 31–98.

Fanale, F. P., T. V. Johnson, and D. L. Matson. 1974. Io: Surface evaporite deposit. *Science*, **186**, 922–925.

Fanale, F. P., T. V. Johnson, and D. L. Matson. 1977. Io's surface and the histories of the Galilean satellites. In: J. A. Burns (ed.), *Planetary Satellites*. University of Arizona Press, Tucson, AZ, pp. 379–405.

Fanale, F. P., R. H. Brown, D. P. Cruikshank, and R. N. Clark. 1979. Significance of absorption features in Io's IR absorption spectrum. *Nature*, **280**, 761–763.

Feaga, L. M., M. A. McGrath, P. D. Feldman, and D. F. Strobel. 2004. Detection of atomic chlorine in Io's atmosphere with the Hubble Space Telescope GHRS. *Astrophys. J.*, **610**, 1191–1198.

Fegley, B. and M. Y. Zolotov. 2000. Chemistry of sodium, potassium, and chlorine in volcanic gases on Io. *Icarus*, **148**, 193–210.

Fink, U., H. P. Larson, L. A. Lebofsky, M. Feierberg, and H. Smith. 1978. The 2–4 μm spectrum of Io. *Bull. Amer. Astron. Soc.*, **10**, 580 (abstract).

Geissler, P. E. 2003. Volcanic activity on Io during the Galileo era. *Annu. Rev. Earth Planet. Sci.*, **31**, 175–211.

Geissler, P. E., A. S. McEwen, L. Keszthelyi, R. Lopes-Gautier, J. Granahan, and D. P. Simonelli. 1999. Global color variations on Io. *Icarus*, **140**, 265–282.

Geissler, P. E., A. McEwen, C. Phillips, L. Keszthelyi, and J. Spencer. 2004. Surface changes on Io during the Galileo mission. *Icarus*, **169**, 29–64.

Granahan, J. C. 2004. The detection of iron sulfide on Io. *Lunar and Planetary Science*, **XXXV**. Lunar and Planetary Institute, Houston, p. 1872.

Hanel, R. A., B. J. Conrath, D. E. Jennings, and R. E. Samuelson. 2003. *Exploration of the Solar System by Infrared Remote Sensing*. Cambridge University Press, Cambridge, UK.

Hapke, B. 1979. Io's surface and environs: A magmatic–volatile model. *Geophys. Res. Lett.*, **6**, 799–802.

Hapke, B. 1989. The surface of Io: A new model. *Icarus*, **79**, 56–74.

Hapke, B. and F. Graham. 1989. Spectral properties of condensed phases of disulfur monoxide, polysulfur oxide, and irradiated sulfur. *Icarus*, **79**, 47–55.

Hapke, B., E. Wells, J. Wagner, and W. Partlow. 1981. Far-UV, visible, and near-IR reflectance spectra of frosts of H_2O, CO_2, NH_3 and SO_2. *Icarus*, **47**, 361–367.

Hopkins, A. G. and C. W. Brown. 1975. Infrared spectrum of sulfur monoxide. *J. Chem. Phys.*, **62**, 2511–2512.

Hopkins, A. G., S.-Y. Tang, and C. W. Brown. 1973. Infrared and Raman spectra of the low-temperature products from discharged sulfur dioxide. *J. Amer. Chem. Soc.*, **95**, 3486–3490.

Hosokawa, S., T. Matsuoka, and K. Tamura. 1994. Optical absorption spectra of liquid sulphur over a wide absorption range. *J. Phys. Condens. Matter*, **6**, 5273–5282.

Howell, R. R., D. P. Cruikshank, and F. P. Fanale. 1984. Sulfur dioxide on Io: Spatial distribution and physical state. *Icarus*, **57**, 83–92.

Howell, R. R., D. B. Nash, T. R. Geballe, and D. P. Cruikshank. 1989. High-resolution infrared spectroscopy of Io and possible surface materials. *Icarus*, **78**, 27–37.

Hunt, G. R., J. W. Salisbury, and C. J. Lenhoff.1974. Visible and near infrared spectra of minerals and rocks. IX: Basic and ultrabasic igneous rocks. *Modern Geology*, **5**, 15–22.

Hunten, D. M., 2003. Sodium at Io. *Nature*, **421**, 30–31.

Jessup, K. L., J. Spencer, G. E. Ballester, R. Yelle, F. Roessler, and R. R. Howell. 2002. Spatially resolved UV spectra of Io's Prometheus plume and anti-Jovian hemisphere. *Bull. Amer. Astron. Soc.*, **34**, 40.02.

Jessup, K. L., J. R. Spencer, and R. Yelle. 2005. Sulfur volcanism on Io. *Bull. Amer. Astron. Soc.*, **37**, 765 (abstract).

Johnson, T. V. and T. McCord. 1970. Galilean satellites: The spectral reflectivity 0.30–1.10 microns. *Icarus*, **13**, 37–42.

Johnson, T. V. and T. B. McCord. 1971. Spectral geometric albedo of the Galilean satellites, 0.3 to 2.5 microns. *Astrophys. J.*, **169**, 589–594.

Johnson, T. V. and C. B. Pilcher. 1977. Satellite spectrophotometry and surface compositions. In: J. A. Burns (ed.), *Planetary Satellites*. University of Arizona Press, Tucson, AZ, pp. 232–268.

Johnson, T. V., G. J. Veeder, D. L. Matson, R. H. Brown, R. M. Nelson, and D. Morrison. 1988. Io: Evidence for silicate volcanism in 1986. *Science*, **242**, 1280–1283.

Kargel, J. S., P. Delmelle, and D. B. Nash. 1999. Volcanogenic sulfur on Earth and Io: Composition and spectroscopy. *Icarus*, **140**, 249–280.

Kargel, J. S., T. MacIntyre, J. B. Dalton, and R. N. Clark. 2000. Io's sulfur: Surface distribution and chemical nature of impurities. *Bull. Amer. Astron. Soc.*, **32**, 29.08 (abstract).

Kargel, J., R. Carlson, A. Davies, B. Fegley Jr., A. Gillespie, R. Greeley, R. R. Howell, K. L. Jessup, L. Kamp, L. Keszthelyi *et al.*, 2003. Extreme volcanism on Io: Latest insights at the end of Galileo Era. *EOS Trans. Amer. Geophys. U.*, **84**, 313, 318.

Keszthelyi, L. and A. McEwen. 1997. Magmatic differentiation on Io. *Icarus*, **130**, 437–448.

Keszthelyi, L., W. L. Jaeger, E. P. Turtle, M. Milazzo, and J. Radebaugh. 2004. A post-Galileo view of Io's interior. *Icarus*, **169**, 271–286.

Khanna, R. K., J. C. Pearl, and R. Dahmani. 1995. Infrared-spectra and structure of solid-phases of sulfur-trioxide: Possible identification of solid SO_3 on Io surface. *Icarus*, **115**, 250–257.

Klaasen, K. P., M. J. S. Belton, H. H. Breneman, A. S. McEwen, M. E. Davies, R. J. Sullivan, C. R. Chapman, G. Neukum, and C. M. Heffernan. 1997. Inflight performance characteristics, calibration, and utilization of the Galileo solid-state imaging camera. *Opt. Eng.*, **36**, 3001–3027.

Kuiper, G. P. 1951. Planetary atmospheres and their origin. In: G. P. Kuiper (ed.), *The Atmospheres of the Earth and Planets*. University of Chicago Press, Chicago, pp. 306–405.

Kuppers, M. and N. M. Schneider. 2000. Discovery of chlorine in the Io torus. *Geophys. Res. Lett.*, **27**, 513–516.

Larson, H. P., R. Timmerman, and U. Fink. 1992. High-resolution observations of the 2.125-μm feature in Io's spectrum during 1975 and 1976. *Icarus*, **95**, 325–328.

Lellouch, E., M. J. S. Belton, I. de Pater, S. Gulkis, and T. Encrenaz. 1990. Io's atmosphere from microwave detection of SO_2. *Nature*, **346**, 639–641.

Lellouch, E., D. F. Strobel, M. J. S. Belton, M. E. Summers, G. Paubert, and R. Moreno. 1996. Detection of sulfur monoxide in Io's atmosphere. *Astrophys. J.*, **459**, L107–L110.

Lellouch, E., G. Paubert, J. I. Moses, N. M. Schneider, and D. F. Strobel, 2003. Volcanically emitted sodium chloride as a source for Io's neutral clouds and plasma torus. *Nature*, **421**, 45–47.

Lester, D. F., L. M. Trafton, T. F. Ramseyer, and N. I. Gaffney. 1992. Discovery of a second narrow absorption feature in the near-infrared spectrum of Io. *Icarus*, **98**, 134–140.

Lewis, J. S. 1982. Io: Geochemistry of sulfur. *Icarus*, **50**, 103–114.

Lo, W.-J., Y.-J. Wu, and Y.-P. Lee. 2002. Isomers of S_2O: Infrared absorption spectra of cyclic S_2O in solid Ar. *J. Chem. Phys.*, **117**, 6655–6661.

Lopes, R. M. C. and D. A. Williams. 2005. Io after Galileo. *Rep. Prog. Phys.*, **68**, 303–340.

Lopes, R. M. C., L. W. Kamp, S. Douté, W. D. Smythe, R. W. Carlson, A. S. McEwen, P. E. Geissler, S. W. Kieffer, F. E. Leader, A. G. Davies, *et al.*, 2001. Io in the near infrared: Near-Infrared Mapping Spectrometer (NIMS) results from the Galileo flybys in 1999 and 2000. *J. Geophys. Res.*, **106**, 33053–33078.

Lopes, R. M. C., L. W. Kamp, W. D. Smythe, P. Mouginis-Mark, J. Kargel, J. Radebaugh, E. P. Turtle, J. Perry, D. A. Williams, R. W. Carlson *et al.* 2004. Lava lakes on Io: Observations of Io's volcanic activity from Galileo NIMS during the 2001 fly-bys. *Icarus*, **169**, 140–174.

Lopes-Gautier, R., S. Douté, W. D. Smythe, L. W. Kamp, R. W. Carlson, A. G. Davies, F. E. Leader, A. S. McEwen, P. E. Geissler, S. W. Kieffer *et al.* 2000. A close-up look at Io from Galileo's near-infrared mapping spectrometer. *Science*, **288**, 1201–1204.

Lunine, J. I., A. Coradini, D. Gautier, T. C. Owen, and G. Wuchterl. 2004. The origin of Jupiter. In: F. Bagenal, T. E. Dowling, and W. McKinnon (eds), *Jupiter: The Planet, Satellites, and Magnetosphere* (Cambridge Planetary Science series). Cambridge University Press, Cambridge, UK, pp. 19–34.

MacIntyre, T., J. S. Kargel, B. Dalton, and R. Clark. 2000. Reflection spectra of impure sulfur: Io and new lab results. *Bull. Amer. Astron. Soc.*, **32**, 30.06, 1049 (abstract).

McEwen, A. S., L. Keszthelyi, J. R. Spencer, G. Schubert, D. L. Matson, R. Lopes-Gautier, K. P. Klaasen, T. V. Johnson, J. W. Head, P. Geissler *et al.* 1998. High-temperature silicate volcanism on Jupiter's moon Io. *Science*, **281**, 87–90.

McEwen, A. S., R. Lopes-Gautier, L. Keszthelyi, and S. W. Kieffer. 2000. Extreme volcanism on Jupiter's moon Io. In: J. Zimbelman and T. Gregg (eds), *Environmental Effects on Volcanic Eruptions: From Deep Oceans to Deep Space*. Kluwer Academic Press/Plenum Publishers, New York, pp. 179–205.

McEwen, A. S., L. P. Keszthelyi, R. Lopes, P. M. Schenk, and J. R. Spencer. 2004. The lithosphere and surface of Io. In: F. Bagenal, T. E. Dowling, and W. B. McKinnon (eds), *Jupiter: The Planet, Satellites, and Magnetosphere* (Cambridge Planetary Science series). Cambridge University Press, Cambridge, UK, pp. 307–328.

McGrath, M. A., M. J. S. Belton, J. R. Spencer, and P. Sartoretti. 2000. Spatially resolved spectroscopy of Io's Pele plume and SO_2 atmosphere. *Icarus*, **146**, 476–493.

McGrath, M. A., E. Lellouch, D. F. Strobel, P. D. Feldman, and R. E. Johnson. 2004. Satellite atmospheres. In: F. Bagenal, T. E. Dowling, and W. B. McKinnon (eds), *Jupiter*. Cambridge University Press, Cambridge, UK, pp. 457–483.

Meyer, B. and T. Stroyer-Hansen. 1972. Infrared spectrum of S_4. *J. Phys. Chem.*, **76**, 3968–3969.

Meyer, B., T. V. Oommen, and D. Jensen. 1971. The color of liquid sulfur. *J. Phys. Chem.*, **75**, 912–917.

Meyer, B., T. Stroyer-Hansen, and T. V. Oommen. 1972. The visible spectrum of S_3 and S_4. *J. Molec. Spectrosc.*, **42**, 335–343.

Moore, M. H. 1984. Studies of proton-irradiated SO_2 at low-temperatures: Implications for Io. *Icarus*, **59**, 114–128.

Morabito, L. A., S. P. Synnott, P. N. Kupferman, and S. A. Collins. 1979. Discovery of currently active extraterrestrial volcanism. *Science*, **204**, 972.

Moreno, M. A., G. Schubert, J. Baumgardner, M. G. Kivelson, and D. A. Paige. 1991. Io's volcanic and sublimation atmospheres. *Icarus*, **93**, 63–81.

Morrison, D. and J. A. Burns. 1976. The Jovian satellites. In: T. Gehrels (ed.), *Jupiter*. University of Arizona Press, Tucson, AZ, pp. 991–1034.

Moses, J. I. and D. B. Nash. 1991. Phase transformations and the spectral reflectance of solid sulfur: Can metastable sulfur allotropes exist on Io? *Icarus*, **89**, 277–304.

Moses, J. I., M. Y. Zolotov, and B. Fegley. 2002. Alkali and chlorine photochemistry in a volcanically driven atmosphere on Io. *Icarus*, **156**, 107–135.

Na, C. Y., L. M. Trafton, E. S. Barker, and S. A. Stern. 1998. A search for new species in Io's extended atmosphere. *Icarus*, **131**, 449–452.

Nash, D. B. 1988. Infrared reflectance spectra of Na_2S with contaminant Na_2CO_3: Effects of adsorbed H_2O and CO_2 and relation to studies of Io. *Icarus*, **74**, 365–368.

Nash, D. B. 1993. A case for Na_2S on Io's surface: Sulfide volcanism? *Io: An International Conference, San Juan Capistrano.*

Nash, D. B. and B. H. Betts. 1995. Laboratory infrared spectra (2.3–23 μm) of SO_2 phases: Applications to Io surface analysis. *Icarus*, **117**, 402–419.

Nash, D. B. and B. H. Betts. 1998. Ices on Io: Composition and texture. In: B. Schmitt, C. de Bergh, and M. Festou (eds), *Solar System Ices. Astrophysics and Space Science Library*. Kluwer, Dordrecht, The Netherlands, pp. 607–638.

Nash, D. B. and F. P. Fanale. 1977. Io's surface composition based on reflectance spectra of sulfur/salt mixtures and proton irradiation experiments. *Icarus*, **31**, 40–80.

Nash, D. B. and R. R. Howell. 1989. Hydrogen sulfide on Io: Evidence from telescopic and laboratory infrared spectra. *Science*, **244**, 454–456.

Nash, D. B. and R. M. Nelson. 1979. Spectral evidence for sublimates and adsorbates on Io. *Nature*, **280**, 763–766.

Nash, D. B., F. P. Fanale, and R. M. Nelson. 1980. SO_2 frost: UV–visible reflectivity and Io surface coverage. *Geophys. Res. Lett.*, 7, 665–668.

Nash, D. B., M. H. Carr, J. Gradie, D. M. Hunten, and C. F. Yoder. 1986. Io. In: J. A. Burns and M. S. Matthews (eds), *Satellites*. University of Arizona Press, Tucson, AZ, pp. 629–688.

Nelson, R. M. and B. W. Hapke. 1978. Spectral reflectivities of the Galilean satellites and Titan, 0.32 to 0.86 micrometers. *Icarus*, **36**, 304–329.

Nelson, R. M., A. L. Lane, D. L. Matson, F. P. Fanale, D. B. Nash, and T. V. Johnson. 1980. Longitudinal distribution of sulfur dioxide frost. *Science*, **210**, 784–786.

Nelson, R. M., A. L. Lane, D. L. Matson, G. J. Veeder, B. J. Buratti, and E. F. Tedesco. 1987. Spectral geometric albedos of the Galilean satellites from 0.24 to 0.34 micrometers: Observations with the International Ultraviolet Explorer. *Icarus*, **72**, 358–380.

Nelson, R. M., W. D. Smythe, B. W. Hapke, and A. J. Cohen. 1990. On the effect of x-rays on the color of elemental sulfur: Implications for Jupiter's satellite Io. *Icarus*, **85**, 326–334.

Nishijima, C., N. Kanamuru, and K. Titmura. 1976. Primary photochemical processes of sulfur in solution. *Bull. Chem. Soc. Japan*, **49**, 1151–1152.

Nyquist, R. A., C. L. Putzig, and M. A. Leugers. 1997. *Infrared and Raman Spectral Atlas of Inorganic Compounds and Organic Salts*. Academic Press, San Diego.

Paranicas, C., B. H. Mauk, R. W. McEntire, and T. P. Armstrong. 2003. The radiation environment near Io. *Geophys. Res. Lett.*, **30**, 1919 SSC 1911–1914.

Peale, S. J., P. Cassen, and R. T. Reynolds. 1979. Melting of Io by tidal dissipation. *Science*, **203**, 892–894.

Pearl, J. 1988. A review of Voyager IRIS results on Io. *Eos, Trans. Amer. Geophys. Union*, **69**, 394 (abstract).

Pearl, J., R. Hanel, V. Kunde, W. Maguire, K. Fox, S. Gupta, C. Ponnamperuma, and F. Raulin. 1979. Identification of gaseous SO_2 and new upper limits for other gases on Io. *Nature*, **280**, 755–758.

Pieri, D. C., S. M. Baloga, R. M. Nelson, and C. Sagan. 1984. Sulfur flows on Ra Patera, Io. *Icarus*, **60**, 685–700.

Pollack, J. B. and F. P. Fanale. 1982. Origin and evolution of the Jovian satellite system. In: D. Morrison (ed.), *Satellites of Jupiter. Space Science Series*. University of Arizona Press, Tucson, AZ, pp. 872–910.

Pollack, J. B., F. C. Witteborn, E. F. Erickson, D. W. Strecker, B. J. Baldwin, and T. E. Bunch. 1978. Near-infrared spectra of the Galilean satellites: Observations and compositional implications. *Icarus*, **36**, 271–303.

Quirico, E., B. Schmitt, R. Bini, and P. R. Salvi. 1996. Spectroscopy of some ices of astrophysical interest: SO_2, N_2, and $N_2:CH_4$ mixtures. *Planet. Space Sci.*, **44**, 973–986.

Radford, H. E. and F. O. Rice. 1960. Green and purple sulfur: Electron spin resonance studies. *J. Chem. Phys.*, **33**, 774–776.

Riskin, Y. I. 1974. The vibrations of protons in minerals: Hydroxyl, water, and ammonium. In: C. V. Farmer (ed.), *The Infrared Spectra of Minerals*. Mineralogical Society, London, pp. 137–181.

Rothschild, W. G. 1964. γ-Ray decomposition of pure liquid sulfur dioxide. *J. Am. Chem. Soc.*, **86**, 1307–1309.

Russell, C. T. (ed.). 1992. *The Galileo Mission* (Space Sci. Rev., Vol. 60). Kluwer, Dordrecht, The Netherlands.

Russell, C. T. and M. G. Kivelson. 2001. Evidence for sulfur dioxide, sulfur monoxide, and hydrogen sulfide in the Io exosphere. *J. Geophys. Res.*, **106**, 33267–33272.

Russell, C. T., J. J. Caldwell, I. de Pater, J. Goguen, M. Klein, B. L. Lutz, N. M. Schneider, W. M. Sinton, and R. A. West. 1990. International Jupiter Watch: A program to study the time variablilty of the Jovian system. *Adv. Space Res.*, **10**, 239–242.

Sagan, C. 1979. Sulfur flows on Io. *Nature*, **280**, 750–753.

Salama, F., L. J. Allamandola, F. C. Witteborn, D. P. Cruikshank, S. A. Sandford, and J. D. Bregman. 1990. The 2.5–5.0-μm spectra of Io: Evidence for H_2S and H_2O frozen in SO_2. *Icarus*, **83**, 66–82.

Salama, F., L. J. Allamandola, S. A. Sandford, J. D. Bregman, F. C. Witteborn, and D. P. Cruikshank. 1994. Is H_2O present on Io? The detection of a new strong band near 3590 cm^{-1} (2.79 μm). *Icarus*, **107**, 413–417.

Salisbury, J. W., L. S. Walter, N. Vergo, and D. M. D'Aria. 1991. *Infrared (2.1–25 μm) Spectra of Minerals* (Johns Hopkins Studies in Earth and Space Science). The Johns Hopkins University Press, Baltimore.

Sandford, S. A. and L. J. Allamandola. 1993. The condensation and vaporization behaviour of ices containing SO_2, H_2S, and CO_2: Implications for Io. *Icarus*, **106**, 478–488.

Sandford, S. A., T. R. Geballe, F. Salama, and D. Goorvitch. 1994. New narrow infrared absorption features in the spectrum of Io between 3600 and 3100 cm^{-1} (2.8–3.2 μm). *Icarus*, **110**, 292–302.

Schaefer, L. and B. Fegley. 2005. Alkali and halogen chemistry in volcanic gases on Io. *Icarus*, **173**, 454–468.

Schmitt, B. and S. Rodriguez. 2000. Tentative identification of a chlorine molecule at Io's surface. *Bull. Amer. Astron. Soc.*, **32**, 29.10.

Schmitt, B. and S. Rodriguez. 2003. Possible identification of local deposits of Cl_2SO_2 on Io from NIMS/Galileo spectra. *J. Geophys. Res.*, **108**, 5104.

Schmitt, B., C. de Bergh, E. Lellouch, J.-P. Maillard, A. Barbe, and S. Douté. 1994. Identification of three absorption bands in the 2-μm spectrum of Io. *Icarus*, **111**, 79–105.

Schmitt, B., C. de Bergh, and M. Festou (eds). 1998a. *Solar System Ices. Astrophysics and Space Science Library*. Kluwer, Dordrecht, The Netherlands.

Schmitt, B., E. Quirica, F. Trotta, and W. M. Grundy. 1998b. Optical properties of ices from the UV to infrared. In: B. Schmitt, C. DeBergh, and M. Festou (eds), *Solar System Ices. Astrophysics and Space Science Library*. Kluwer, Dordrecht, The Netherlands, pp. 199–240.

Schriver, A., L. Schriver, and J. P. Perchard. 1988. Infrared matrix isolation studies of complexes between water and sulfur dioxide: Identification and structure of the 1:1, 1:2, and 2:1 species. *J. Molec. Spect.*, **127**, 125–142.

Schubert, G., J. D. Anderson, T. Spohn, and W. B. McKinnon. 2004. Interior composition, structure, and dynamics of the Galilean satellites. In: F. Bagenal, T. E. Dowling, and W. McKinnon (eds), *Jupiter: The Atmosphere, Satellites, and Magnetosphere*. Cambridge Univ. Press, Cambridge, UK, pp. 281–306.

Sill, G. T. 1973. Reflectance spectra of solids of planetary interest. *Comm. Lunar Planet. Lab.*, **10**, 1–7.

Sill, G. T. and R. N. Clark. 1982. Composition of the surfaces of the Galilean satellites. In: D. Morrison (ed.), *Satellites of Jupiter*. University of Arizona Press, Tucson, AZ, pp. 174–212.

Simonelli, D. P., J. Boucher, P. Helfenstein, J. Veverka, and M. O'Shaughnessy. 1994. Search for temperature-related albedo changes in nightside and posteclipse images. *Icarus*, **107**, 375–387.

Sinton, W. M., D. Lindwall, F. Cheigh, and W. C. Tittemore. 1983. Io: The Near-infrared Monitoring Program, 1979–1981. *Icarus*, **54**, 133–157.

Smythe, W. D., R. M. Nelson, and D. B. Nash. 1979. Spectral evidence for SO_2 frost or adsorbate on Io's surface. *Nature*, **280**, 766.

Smythe, W. D., R. Lopes-Gautier, S. Douté, S. W. Kieffer, R. W. Carlson, L. Kamp, and F. Leader. 2000. Evidence for massive sulfur dioxide deposit on Io. *Bull. Amer. Astron. Soc.*, **32**, 1047–1048.

Spencer, J. R. and N. M. Schneider. 1996. Io on the Eve of the Galileo Mission. *Annu. Rev. Earth Planet. Sci.*, **24**, 125–190.

Spencer, J. R., W. M. Calvin, and M. J. Person. 1995. Charge-coupled-device spectra of the galilean satellites: Molecular-oxygen on Ganymede. *J. Geophys. Res.*, **100**, 19049–19056.

Spencer, J. R., A. S. McEwen, M. A. McGrath, P. Sartoretti, D. B. Nash, K. S. Noll, and D. Gilmore. 1997. Volcanic resurfacing of Io: Post-repair HST imaging. *Icarus*, **127**, 221–237.

Spencer, J. R., K. L. Jessup, M. A. McGrath, G. E. Ballester, and R. Yelle. 2000. Discovery of gaseous S_2 in Io's Pele plume. *Science*, **288**, 1208–1210.

Spencer, J. R., R. W. Carlson, T. L. Becker, and J. S. Blue. 2004. Maps and spectra of Jupiter and the Galilean satellites. In: F. Bagenal, T. E. Dowling, and W. B. McKinnon (eds), *Jupiter: The Planet, Satellites, and Magnetosphere*. Cambridge University Press, Cambridge, UK, pp. 689–698.

Steudel, R. (ed.). 2003a. *Elemental Sulfur and Sulfur-Rich Compounds. I: Top. Curr. Chem.*, **230**. Springer, Berlin.

Steudel, R. (ed.). 2003b. *Elemental Sulfur and Sulfur-Rich Compounds. II: Top. Curr. Chem.*, **231**. Springer, Berlin.

Steudel, R. 2003c. Sulfur-rich oxides S_nO and S_nO_2 ($n > 1$). *Top. Curr. Chem.*, **231**, 203–230.

Steudel, R. and Y. Steudel. 2004. The thermal decomposition of S_2O forming SO_2, S_3, S_4, and S_5O: An ab initio MO study. *Eur. J. Inorg. Chem.*, **2004**, 3513–3521.

Steudel, R., G. Holdt, and A. T. Young. 1986. On the colors of Jupiter's satellite Io: Irradiation of solid sulfur at 77 K. *J. Geophys. Res.*, **91**, 4971–4977.

Steudel, R., Y. Steudel, and M. W. Wong. 2003. Speciation and thermodynamics of sulfur vapor. *Top. Curr. Chem.*, **230**, 117–134.

Thomas, N., F. Bagenal, T. W. Hill, and J. K. Wilson. 2004a. The Io neutral clouds and plasma torus. In: F. Bagenal, T. E. Dowling, and W. McKinnon (eds), *Jupiter*. Cambridge University Press, Cambridge, UK, pp. 561–592.

Thomas, N., F. Bagenal, T. W. Hill, and J. K. Wilson. 2004b. The Io neutral clouds and plasma torus. In: F. Bagenal, T. E. Dowling, and W. McKinnon (eds), *Jupiter: The Planet, Satellites, and Magnetosphere*. Cambridge University Press, Cambridge, UK, pp. 561–591.

Trafton, L., D. F. Lester, T. F. Ramseyer, F. Salama, S. A. Sandford, and L. J. Allamandola. 1991. A new class of absorption features in Io's near-infrared spectrum. *Icarus*, **89**, 264–276.

Voegele, A. F., T. Loerting, C. S. Tautermann, A. Hallbrucker, E. Mayer, and K. R. Liedl. 2004. Sulfurous acid (H_2SO_3) on Io? *Icarus*, **169**, 242–249.

Wagner, J., B. Hapke, and E. Wells. 1987. Atlas of reflectance spectra of terrestrial, lunar, and meteoritic powders and frosts from 92 to 1800 nm. *Icarus*, **69**, 14–28.

Wamsteker, W., R. L. Kroes, and J. A. Fountain. 1973. On the surface composition of Io. *Icarus*, **23**, 417–424.

Williams, D. A., J. Radebaugh, L. P. Keszthelyi, A. S. McEwen, R. M. C. Lopes, S. Douté, and R. Greeley. 2002. Geologic mapping of the Chaac–Camaxtli region of Io from Galileo imaging data. *J. Geophys. Res.*, **107**, doi:10.1029/2001JE001821.

Witteborn, F. C., J. C. Bregman, and J. P. Pollack. 1979. Io: An intense brightening near 5 micrometers. *Science*, **203**, 643–646.

Wong, M. C. and R. E. Johnson. 1996a. A three-dimensional azimuthally symmetric model atmosphere for Io. 1: Photochemistry and the accumulation of a nightside atmosphere. *J. Geophys. Res.*, **101**, 23243–23254.

Wong, M. C. and R. E. Johnson. 1996b. A three-dimensional azimuthally symmetric model atmosphere for Io. 2: Plasma effect on the surface. *J. Geophys. Res.*, **101**, 23255–23259.

Young, A. T., 1984. No sulfur flows on Io. *Icarus*, **58**, 197–226.

Zhang, J., D. B. Goldstein, P. L. Varghese, N. E. Gimelshein, S. F. Gimelshein, and D. A. Levin. 2003. Simulation of gas dynamics and radiation in volcanic plumes on Io. *Icarus*, **163**, 182–197.

Zolotov, M. Y. and B. Fegley. 1998. Volcanic production of sulfur monoxide (SO) on Io. *Icarus*, **132**, 431–434.

Zolotov, M. Y. and B. Fegley. 2000. Eruption condition of Pele volcano on Io inferred from chemistry of its volcanic plume. *Geophys. Res. Lett.*, **27**, 2789–2792.

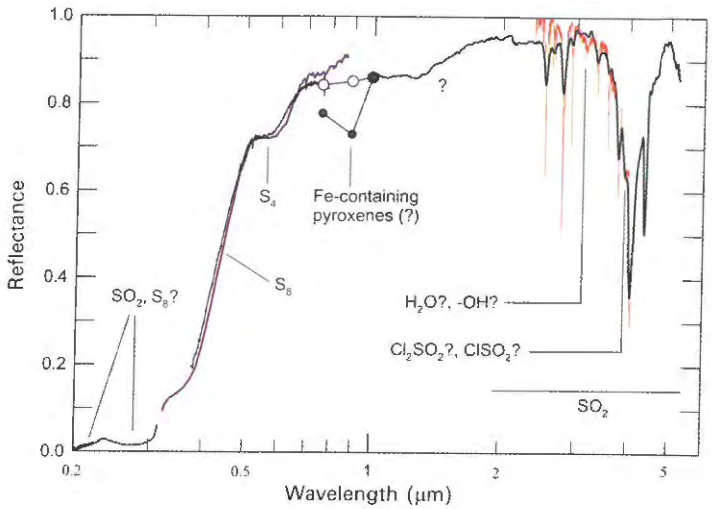

Figure 9.1. Solar reflectance spectra of Io. The ultraviolet HST measurements in the 200- to 310-nm region are from Jessup *et al.* (2002); ground-based measurements from 330–860-nm data (blue line) and from 380–780 nm (black line) are from Nelson and Hapke (1978) and Spencer *et al.* (1995), respectively. Scaled *Galileo* SSI multicolor spectrophotometry of white areas (open circles) and dark areas (filled circles) are from Geissler *et al.* (1999). Modest resolution near-infrared measurements by *Galileo* NIMS (black line) are from Carlson *et al.* (1997) while the higher resolution ISO spectrum (red line) is from Schmitt and Rodriguez (2003). Many of these spectra are summarized in the compilation by Spencer *et al.* (2004).

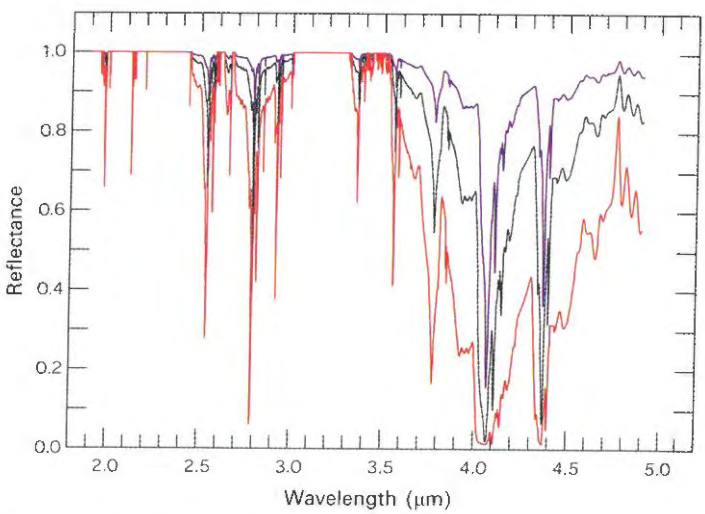

Figure 9.6. Theoretical reflectance spectra for SO_2 frost. The diffuse reflectance spectra of optically thick frosts of 10-, 100-, and 1,000-μm grains are shown as blue, black, and red lines, respectively. The optical constants of Schmitt *et al.* (1994, 1998b) were used.

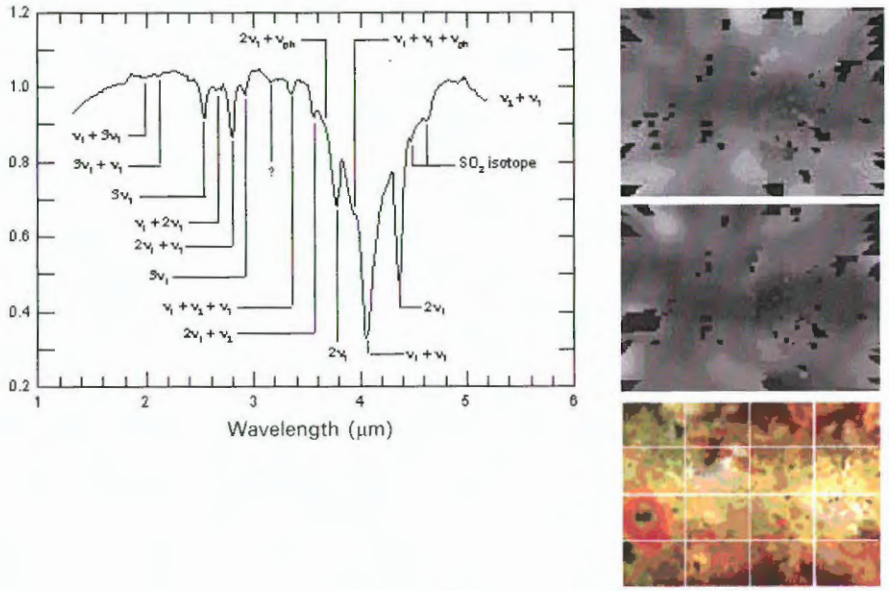

Figure 9.7. Spectrum of Io and equivalent-width maps. Maps of the absorption strength (equivalent width) of the 1.98-μm SO_2 band (*top*) and the 3.15-μm band (*middle*) are shown at the right, with black signifying more absorption. Note the strong equatorial enhancement of the unknown 3.15-μm absorber (possibly H_2O) and its correlation with both the weak, long-path-length SO_2 feature and the bright deposits in the Io reference map (*bottom*).

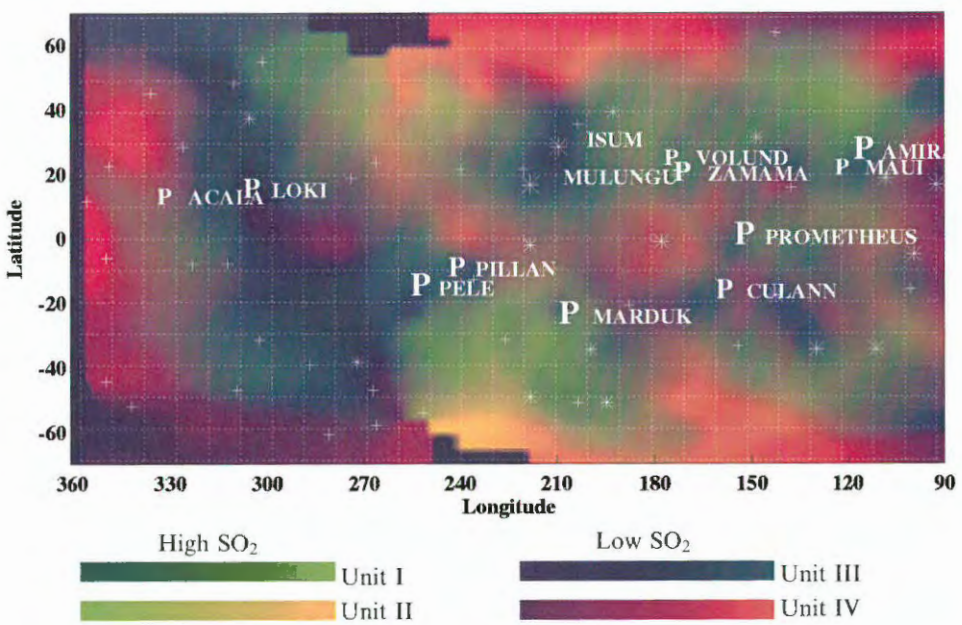

Figure 9.8. Sulfur dioxide spectral unit map. The plumes (P) are sources of fine-grained SO_2 frost (Unit I, green) deposits, generally poleward of the low-latitude plumes. Hot spot locations are denoted with stars and crosses, with stars being long-lived hot spots and crosses denoting sporadic thermal features. Metamorphosed SO_2 snowfields (Unit II) are shown as light green and yellow. SO_2-poor areas (Units III, IV) occur in the 270 to >360°W longitude region.